JPRS-JST-90-039
21 AUGUST 1990

FOREIGN BROADCAST INFORMATION SERVICE

JPRS Report

Science & Technology

Japan

89 SAIRAS SYMPOSIUM

JPRS-JST-90-039
21 AUGUST 1990

SCIENCE & TECHNOLOGY

JAPAN

89 SAIRAS SYMPOSIUM

906C0047 Tokyo SAIRAS 89 PROCEEDINGS in Japanese 18-19 Oct 89
pp 1-271

[Selected articles from the Proceedings of the Space Artificial Intelligence/Robotics/Automation Symposium '89 held 18-19 Oct 89 in Tokyo, sponsored by the Japan Aeronautics and Space Institute, Artificial Intelligence Institute, Japan Robotics Institute, National Aerospace Laboratory, STA, National Space Development Agency of Japan, and Institute of Space and Astronautical Science.]

CONTENTS

Japan/U.S.A. Sessions Program..... 1

Japanese Sessions Program..... 3

Contents..... 5

Control of Space Robots in Capturing Tumbling Objects
[Z. H. Luo, Y. Sakawa]..... 7

Configuration of Manipulator Control System for Space Robots
[Kenji Ogimoto, Osamu Miki, et al.]..... 16

Development of Target Capturing Device With Flexible Capability
[Yoshitugu Toda, Kazuo Machida, et al.]..... 23

Capture of Free-Flying Target Using Visual Information
[H. Shimoji, M. Inoue, et al.]..... 28

A Study on Functional Allocation of Robot Systems in Orbit
[Yuuki Yoshie, Fumiaki Sano]..... 36

A Teleoperating Assembly System
[Hajime Morikawa, Nobuaki Takanashi, et al.]..... 42

JAPAN/U.S.A. Sessions Program

October, 18· Wednesday

[PLENARY] 9:30a.m.–10:40a.m.

Session Chairmen : Keiken Ninomiya (ISAS)
Lee B. Holcomb (NASA HQ's)

A1–1 Welcome Address (9:30a.m.–9:40a.m.)
Yoji Umetani (Tokyo Institute of Technology)

A1–2 Keynote Address (9:40a.m.–10:40a.m.)
NASA's Automation and Robotics Research Program
Melvin D. Montemerlo (NASA HQ's)

[OVERVIEW(1)] 10:50a.m.–12:05p.m.

Session Chairmen : Ichiro Nakatani (ISAS)
Lee B. Holcomb (NASA HQ's)

A1–3 NASDA A & R Activities
Tsutomu Iwata (NASDA Tsukuba Space Center)

A1–4 Telerobotic Research for In–Space Structural Assembly and Servicing
Alfred J.Meintel, Jr. (NASA LaRC)

A1–5 Space Robotics Researches at ElectroTechnical Laboratory
Masatoshi Ono, Kazuo Machida, Shigeoki Hirai
(ElectroTechnical Laboratory, MITI)

[SYSTEM CONCEPT(1)] 1:30p.m.–2:45p.m.

Session Chairmen : Kiyoshi Ueno (JSUP)
Melvin D. Montemerlo (NASA HQ's)

A1–6 COSMO–LAB Project Proposed by Space Robotics Forum
Yoji Umetani (Tokyo Institute of Technology)

A1–7 Robots for Assembling a Space Laboratory
Hironori Fujii (Tokyo Metropolitan Institute of Technology)

A1–8 The Role of Robotics in the Space Experiment
Kohtaro Matsumoto, Seisiroh Kibe (National Aerospace Laboratory, STA)

[SYSTEM CONCEPT(2)] 2:55p.m.–4:35p.m.

Session Chairmen : Mitsushige Oda (NASDA)
Melvin D. Montemerlo (NASA HQ's)

A1–9 The servicing of Eureca Type Platforms at The Space Station in preparation of Columbus Servicing Technologies
R. Boudreault (Oerlikon Aerospace Inc.)
J. Criswick, J. Bradley (Canadian Astronautics Limted)
P.Kumar (Opsys Engineering Limited)
S.Ransom, J. Weydandt, W. Rath (MBB/ERNO)

A1–10 Is Lobster More Dextorous Than Crab ?
Yoji Umetani, Kazuya Yoshida (Tokyo Institute of Technology)

A1–11 Robotic Application to Telecommunication
Tetsuo Yasaka, Yoichi Kawakami,
Yoshihiko Nomura, Tetsuro Yabuta
(NTT Electrical Communication Laboratories)

[TEST BED] 4:45p.m.–6:00p.m.

Session Chairmen : Osamu Okamoto (NAL)
Melvin D. Montemerlo (NASA HQ's)

A1–12 NASA's Telerobotic Testbed
John F. Stocky (JPL)

A1–13 Concept of a Testbed Model for The 2nd generation Space Robot
Tsutomu Iwata, Mitsushige Oda, Taichi Nakamura
(NASDA Tsukuba Space Center)

A1–14 FTS simulator : Preparing for The Flight Telerobotic Servicer
David E. Provost (NASA GSFC)

[Reception] (18:15 20:20)

October, 19 Thursday

[OVERVIEW(2)] 9:30a.m.–10:45a.m.

Session Chairmen : Tsutomu Iwata (NASDA)
Peter Friedland (NASA ARC)

A2–1 Robotic Applications for Launch Vehicle Ground Processing
T. Davis, D. Davis (NASA KSC)
D.Wegerif, M. Sklar (McDonnell Douglas Space Systems Company)

A2–2 Space Robotics Research in MEL
Tsuneji Yada, Susumu Tachi, Kazuo Tanie
(Mechanical Engineering Laboratory,MITI)

A2–3 Artificial Intelligence Research at NASA Ames Research Center
Peter Friedland (NASA ARC)

[OVERVIEW(3)]11:00a.m.–11:50a.m.

Session Chairmen : Tetsuo Yasaka(NTT)
Peter Friedland (NASA ARC)

A2–4 Research Activities on Space Robotics and Automation at National Aerospace Laboratory (NAL)
Yoshiaki Ohkami (National Aerospace Laboratory, STA)

A2–5 The Systems Autonomy Technology Program: Today's Research for Tomorrow's Space Station
Kathleen J.Healey (NASA JSC)

[CONTROL & MANIPULATOR] 1:20p.m.–3:00p.m.

Session Chairmen : Yoshiaki Ohkami (NAL)
John F. Stocky (JPL)

A2–6 Force Torque Control for The Space Shuttle Remote Manipulator System
Charles R.Price (NASA JSC)

A2–7 Fuzzy Control of Space Manipulators using Neural Network Techniques
Toshiaki Iwata (ElectroTechnical Laboratory, MITI)
Neil A. Duffie (Univ.of Wisconsin)

A2–8 Analysis of Space Manipulator System in Ground Simulation
Hironori Fujii, Kenji Uchiyama, Kohji Sakemi
(Tokyo Metropolitan Institute of Technology)
Takashi Uchiyama (Fujitsu Laboratories Ltd.)
Tatsuo Mikami (Fujitsu Ltd.)

A2–9 Fuzzy Logic Approach to Combined Translational and Rotational Control of a Spacecraft in Proximity of The Space Station
Robert N. Lea (NASA JSC)
Masaki Togai, Jon Teichrow (Togai InfraLogic Inc.)
Yashvant Jani (LinCom Corp.)

[ARTIFICIAL INTELLIGENCE] 3:20p.m.–5:00p.m.

Session Chairmen : Kohtaro Matsumoto (NAL)
John F. Stocky (JPL)

A2–10 Artificial Intelligence for Multi–Mission Planetary Spacecraft Operations
David J. Atkinson, Denise L. Lawson, Mark L. James (JPL)

A2–11 Research on Plan–based Intelligent Agent Architrectures
Mark Drummond (NASA ARC)

A2–12 Design of and Reasoning about Engineered Systems
Monte Zweben (NASA ARC)

A2–13 Model–based Reasoning for Space Applications
Richard J. Doyle (JPL)

Japanese Sessions Program

October 18, Wednesday

[Expert System] 10:50a.m.–12:30p.m. Chairman : Atsuhiro Takasu (NACSIS)

B1–1 A Diagnostic Expert System for Environment Control Equipment in Space (Part)
Nobuyoshi Muroi, Yoshimitsu Kurosaki, Yuichi Miyamoto, Hiroaki Fujimori, Ikuo Akeyama, Toshiaki Ueda, Nobuhisa Maeno (Kawasaki Heavy Industries)

B1–2 Fault Diagnosis Expert System for JEM Power System
Eiichi Ogawa, Shigeki Kuzuoka, Keinosuke Matsumoto (Mitsubishi Electric)

B1–3 Spacecraft orbital Operation support System (SOS)
Tsutomu Nakajima, Noriko Aso, Mika Hiwatashi, Masuko Yamaguchi (Mitsubishi Electric)

B1–4 Approximate Reasoning System Based on Fuzzy Logic and Dempster–Shafer's Theory
Tohru Shimizu (NEC)

[Manipulator Control (1)] 13:30p.m.–15:10p.m. Chairman : Kazuo Machida (ETL)

B1–5 Control of Space Robots for Capturing a Tumbling Object
Z. H. LUO, Y.Sakawa (Osaka Univ.)

B1–6 Control of a 2–link Flexible Arm
Akihiro Maekawa, Yukio Tanaka, Takeya Kawamura, Shinya Ishii (Mitsubishi Heavy Industries)

B1–7 Configuration of Manipulator Control System for Space Robots
Kenji Ogimoto, Osamu Miki, Osamu Noro, Kiyoshi Ioi, Nobuyoshi Muroi (Kawasaki Heavy Industries)

B1–8 Manipulator Trajectories Generated by Virtual Hinge Forces
Osamu Okamoto, Yoshiaki Ohkami, Takashi Kida, Isao Yamaguchi (National Aerospace Laboratory, STA)

[Manipulator Control (2)] 15:20p.m.–17:00p.m. Chairman : Hironori Fujii (TMIT)

B1–9 Motion Analysis of Space Manipulator with taking Every Link Mass and Inertial Tensor into Account
Mitsushige Oda (NASDA)
Masataka Ajiro, Manabu Yatabe (Mitsubishi Space Software)

B1–10 Development of Target Capturing Device with Flexible Capability
Yoshitugu Toda, Kazuo Machida, Toshiaki Iwata (ElectroTechnical Lab.)
Shouichi Iikura, Tadashi Komatsu, Masaru Oka, Toshio Honda (Toshiba)

B1–11 Consideration on Simulator for Free–Flying Motion
Osamu Miki, Osamu Noro, Kiyoshi Ioi, Ryuuji Sakata, Nobuyoshi Muroi (Kawasaki Heavy Industries)

B1–12 Capture of Free–Flying Target Using Visual Information
H. Shimoji, M. Inoue, K. Tsuchiya (Mitsubishi Electric)
K. Ninomiya, I. Nakatani, J. Kawaguchi (ISAS)

October 19, Thursday

[System Concept] 9:30a.m.–10:20a.m. Chairman : Yukihiro Sakawa (Osaka Univ.)

B2–1 A Study on Functional Allocation of Robot Systems in Orbit
Yuuki Yoshie, Fumiaki Sano (Ishikawajima–Harima Heavy Industries)

B2–2 Preliminary Study on Autonomous Onboard Data Management & Handling System for Space Platform
Hiroshi Anegawa, Hiroshi Arikawa (NASDA)

[Vision System] 10:35a.m.–11:50a.m. Chairman : Masao Naka (NAL)

B2–3 Teleoperated Orbital Operation Experiment System
Hiroshi Koyama,Yukiko Yoshimoto, Norimasa Yoshida, Masao Inoue, Haruhiko Shimoji, Kazuyoshi Yabuuchi (Mitsubishi Electric)

B2–4 Visual Information Processing for Space Robot Teleoperation
Eiichi Ogawa, Shigeki Kuzuoka (Mitsubishi Electric)

B2–5 Region Segmentation Process for Visual Data
Mikio Fukase, Tsugito Maruyama, Takashi Uchiyama (Fujitsu Labs.)
Osamu Okamoto, Isao Yamaguchi (NAL)

[Rendezvous and Docking] 1:20p.m.–2:10p.m. chairman : Tomomasa Satou (ETL)

B2–6 Computer Simulation of Docking and Berthing Motion between Two Space Vehicles
Hidehiko Mitsuma,Eiichi Endo, (NASDA)
Nobuyuki Kubota,Kiyoshi Ioi,Toshiyuki Itoko, Tetsuya Kubota, Nobuyoshi Muroi (Kawasaki Heavy Industries)

B2–7 Bilateral Guidance of Free Flying Telerobot Using Proximity Sensor
Kazuo Machida, Yoshitugu Toda (ETL)
Michihiro Uenohara (Toshiba)

[Tele–Operation] 2:30p.m.–4:35p.m. Chairman : Susumu Tachi (MEL)

B2–8 Simulation of Teleoperated EVA Robots (2nd Rep.)
Yasuhiro Masutani, Fumio Miyazaki (Osaka Univ.)

B2–9 Experimental Test Bed for Telescience
Ichiro Watanabe, Keiju Okabayashi, Ryosuke Suda, Syozo Fujita, Takashi Uchiyama (Fujitsu Lab.)
Seiichi Fujii, Kaoru Tsumura, Hiroshi Hirakawa (Fujitsu)

B2–10 canceled

B2–11 Intelligent Telerobot System – Operational Support by Graphics and Audio–
Shigeoki Hirai, Tomomasa Sato (ETL)
Tadao Hiruma (Meiji Univ.)

B2–12 A Teleoperating Assembly System
Hajime Morikawa, Nobuaki Takanashi, Norio Tagawa, Hiromichi Fukuchi (NEC)

CONTENTS

A1–2 NASA's Automation and Robotics Research Program 16
Melvin D. Montemerlo (NASA HQ's)
A1–3 NASDA A & R Activities 24
Tsutomu Iwata (NASDA Tsukuba Space Center)
A1–4 Telerobotic Research for In–Space Structural Assembly and Servicing 28
Alfred J.Meintel, Jr. (NASA LaRC)
A1–5 Space Robotics Researches at ElectroTechnical Laboratory 36
Masatoshi Ono, Kazuo Machida, Shigeoki Hirai
(ElectroTechnical Laboratory, MITI)
A1–6 COSMO–LAB Project Proposed by Space Robotics Forum 44
Yoji Umetani (Tokyo Institute of Technology)
A1–7 Robots for Assembling a Space Laboratory 48
Hironori Fujii (Tokyo Metropolitan Institute of Technology)
A1–8 The Role of Robotics in the Space Experiment 52
Kohtaro Matsumoto, Seisiroh Kibe (National Aerospace Laboratory, STA)
A1–10 Is Lobster More Dextorous Than Crab ? 60
Yoji Umetani, Kazuya Yoshida (Tokyo Institute of Technology)
A1–11 Robotic Application to Telecommunication 64
Tetsuo Yasaka, Yoichi Kawakami,
Yoshihiko Nomura, Tetsuro Yabuta
(NTT Electrical Communication Laboratories)
A1–12 NASA's Telerobotic Testbed 72
John F. Stocky (JPL)
A1–13 Concept of a Testbed Model for The 2nd generation Space Robot 78
Tsutomu Iwata, Mitsushige Oda, Taichi Nakamura
(NASDA Tsukuba Space Center)
A1–14 FTS simulator : Preparing for The Flight Telerobotic Servicer 82
David E. Provost (NASA GSFC)
A2–1 Robotic Applications for Launch Vehicle Ground Processing 90
T. Davis, D. Davis (NASA KSC)
D.Wegerif, M. Sklar (McDonnell Douglas Space Systems Company)
A2–2 Space Robotics Research in MEL 94
Tsuneji Yada, Susumu Tachi, Kazuo Tanie
(Mechanical Engineering Laboratory,MITI)
A2–3 Artificial Intelligence Research at NASA Ames Research Center 98
Peter Friedland (NASA ARC)
A2–4 Research Activities on Space Robotics and Automation at National Aerospace Laboratory (NAL) 104
Yoshiaki Ohkami (National Aerospace Laboratory, STA)
A2–5 The Systems Autonomy Technology Program: Today's Research for Tomorrow's Space Station 106
Kathleen J.Healey (NASA JSC)
A2–6 Force Torque Control for The Space Shuttle Remote Manipulator System 114
Charles R.Price (NASA JSC)
A2–7 Fuzzy Control of Space Manipulators using Neural Network Techniques 118
Toshiaki Iwata (ElectroTechnical Laboratory, MITI)
Neil A. Duffie (Univ.of Wisconsin)
A2–8 Analysis of Space Manipulator System in Ground Simulation 122
Hironori Fujii, Kenji Uchiyama, Kohji Sakemi
(Tokyo Metropolitan Institute of Technology)
Takashi Uchiyama (Fujitsu Laboratories Ltd.)
Tatsuo Mikami (Fujitsu Ltd.)
A2–9 Fuzzy Logic Approach to Combined Translational and Rotational Control of a Spacecraft in Proximity of The Space Station 126
Robert N. Lea (NASA JSC)
Masaki Togai, Jon Teichrow (Togai InfraLogic Inc.)
Yashvant Jani (LinCom Corp.)

A2–10 Artificial Intelligence for Multi–Mission Planetary Spacecraft Operations 136
David J. Atkinson, Denise L. Lawson, Mark L. James (JPL)
A2–11 Research on Plan–based Intelligent Agent Architectures 140
Mark Drummond (NASA ARC)
A2–12 Design of and Reasoning about Engineered Systems 144
Monte Zweben (NASA ARC)
A2–13 Model–based Reasoning for Space Applications 148
Richard J. Doyle (JPL)
B1–1 A Diagnostic Expert System for Environment Control Equipment in Space (Part) 156
Nobuyoshi Muroi, Yoshimitsu Kurosaki, Yuichi Miyamoto, Hiroaki Fujimori, Ikuo Akeyama, Toshiaki Ueda, Nobuhisa Maeno (Kawasaki Heavy Industries)
B1–2 Fault Diagnosis Expert System for JEM Power System 160
Eiichi Ogawa, Shigeki Kuzuoka, Keinosuke Matsumoto (Mitsubishi Electric)
B1–3 Spacecraft orbital Operation support System (SOS) 164
Tsutomu Nakajima, Noriko Aso, Mika Hiwatashi, Masuko Yamaguchi (Mitsubishi Electric)
B1–4 Approximate Reasoning System Based on Fuzzy Logic and Dempster–Shafer's Theory 168
Tohru Shimizu (NEC)
B1–5 Control of Space Robots for Capturing a Tumbling Object 176
Z. H. LUO, Y.Sakawa (Osaka Univ.)
B1–6 Control of a 2–link Flexible Arm 180
Akihiro Maekawa, Yukio Tanaka, Takeya Kawamura, Shinya Ishii (Mitsubishi Heavy Industries)
B1–7 Configuration of Manipulator Control System for Space Robots 184
Kenji Ogimoto, Osamu Miki, Osamu Noro, Kiyoshi Ioi, Nobuyoshi Muroi (Kawasaki Heavy Industries)
B1–8 Manipulator Trajectories Generated by Virtual Hinge Forces 188
Osamu Okamoto, Yoshiaki Ohkami, Takashi Kida, Isao Yamaguchi (National Aerospace Laboratory, STA)
B1–9 Motion Analysis of Space Manipulator with taking Every Link Mass and Inertial Tensor into Account 194
Mitsushige Oda (NASDA)
Masataka Ajiro, Manabu Yatabe (Mitsubishi Space Software)
B1–10 Development of Target Capturing Device with Flexible Capability 198
Yoshitugu Toda, Kazuo Machida, Toshiaki Iwata (ElectroTechnical Lab.)
Shouichi Iikura, Tadashi Komatsu, Masaru Oka, Toshio Honda (Toshiba)
B1–11 Consideration on Simulator for Free–Flying Motion 202
Osamu Miki, Osamu Noro, Kiyoshi Ioi, Ryuuji Sakata, Nobuyoshi Muroi (Kawasaki Heavy Industries)
B1–12 Capture of Free–Flying Target Using Visual Information 206
H. Shimoji, M. Inoue, K. Tsuchiya (Mitsubishi Electric)
K. Ninomiya, I. Nakatani, J. Kawaguchi (ISAS)
B2–1 A Study on Functional Allocation of Robot Systems in Orbit 214
Yuuki Yoshie, Fumiaki Sano (Ishikawajima–Harima Heavy Industries)
B2–2 Preliminary Study on Autonomous Onboard Data Management & Handling System for Space Platform 218
Hiroshi Anegawa, Hiroshi Arikawa (NASDA)
B2–3 Teleoperated Orbital Operation Experiment System 226
Hiroshi Koyama, Yukiko Yoshimoto, Norimasa Yoshida, Masao Inoue, Haruhiko Shimoji, Kazuyoshi Yabuuchi (Mitsubishi Electric)
B2–4 Visual Information Processing for Space Robot Teleoperation 230
Eiichi Ogawa, Shigeki Kuzuoka (Mitsubishi Electric)
B2–5 Region Segmentation Process for Visual Data 234
Mikio Fukase, Tsugito Maruyama, Takashi Uchiyama (Fujitsu Labs.)
Osamu Okamoto, Isao Yamaguchi (NAL)
B2–6 Computer Simulation of Docking and Berthing Motion between Two Space Vehicles 242
Hidehiko Mitsuma,Eiichi Endo, (NASDA)
Nobuyuki Kubota,Kiyoshi Ioi,Toshiyuki Itoko, Tetsuya Kubota, Nobuyoshi Muroi (Kawasaki Heavy Industries)
B2–7 Bilateral Guidance of Free Flying Telerobot Using Proximity Sensor 246
Kazuo Machida, Yoshitugu Toda (ETL)
Michihiro Uenohara (Toshiba)
B2–8 Simulation of Teleoperated EVA Robots (2nd Rep.) 252
Yasuhiro Masutani, Fumio Miyazaki (Osaka Univ.)
B2–9 Experimental Test Bed for Telescience
Ichiro Watanabe, Keiju Okabayashi, Ryosuke Suda, Syozo Fujita, Takashi Uchiyama (Fujitsu Lab.)
Seiichi Fujii, Kaoru Tsumura, Hiroshi Hirakawa (Fujitsu)
B2–11 Intelligent Telerobot System – Operational Support by Graphics and Audio – 260
Shigeoki Hirai, Tomomasa Sato (ETL)
Tadao Hiruma (Meiji Univ.)
B2–12 A Teleoperating Assembly System 264
Hajime Morikawa, Nobuaki Takanashi, Norio Tagawa, Hiromichi Fukuchi (NEC)

Control of Space Robots in Capturing Tumbling Objects

906C0047A Tokyo SAIRAS 89 PROCEEDINGS in Japanese 18-19 Oct 89 pp 176-179

[Article by Z. H. Luo and Y. Sakawa, Dept of Control Engineering, Faculty of Engineering Sciences, Osaka University]

[Text] Abstract

A space robot consists of two parts, namely a satellite base and a manipulator mounted on the base. Unlike the earth-mounted robots (EMR), any motion of the satellite-mounted manipulator (SMM) will cause the motion of the satellite base, and vice versa. Hence the motions of the two parts are highly coupled. Control of SMM thus becomes much more difficult than that of EMR.

Longman etc.[1] discussed the kinematics and reaction moment compensation problems of SMM. Their techniques are essentially forward, or say, open loop scheme. Umetani and Yoshida[2] proposed the so-called "Generalized Jacobian Method (GJM)" to control SMM. This method strongly relies on both the linear and angular momentum conservations. Masutani etc.[4] and Tsuchiya and Yamada[5] used the idea of GJM And successfully realized sensor feedback controllers for the position and orientation control of SMM.

All these works intended to generalize the well known results for EMR to the control of SMM. However, one should recognize that the space environment is quite different from the earth environment. For example, a satellite may be subject to very complex motions. In this case, GJM is not always applicable. Let us also point out that it is not an easy task to evaluate the generalized Jacobian.

Keeping these in mind, we shall consider in this work the dynamics and control of the SMM with an active control of the satellite base. During the manipulation, the total external forces are assumed to be 0, but the torques are applied to change the angular momentum, hence only linear momentum conservation holds. The problem is to capture a torque-free axisymmetric body, which is undergoing tumbling motion in space environment. A Lyapunov approach is applied to derive control torques which guarantee that the position and orientation of the manipulator hand will approach that of the body to be captured. To implement the proposed control law, we need essentially the information about the position and orientation of the object measured from

the satellite base, the information of the orientation of the satellite base measured from the inertial coordinate system, and the information of the position and orientation of the object measured from the hand coordinate system.

1. Introduction

Beginning with the space station project by NASA, an age of space utilization is just about to start on a full scale. Space robots are expected to play a big role in the fields of assembling structures in space, maintenance and recovery of satellites. However, in comparison with earth-mounted robots (EMR) based on the ground, the base of satellite-mounted manipulators is more free to move at will causing it to be much more difficult to control robots in space. Our study here will describe dynamics of a robot and its control method in controlling actively and simultaneously the attitude of a satellite main unit and joint angles of its robot.

2. Dynamic Model

A space robot as shown in Fig. 1 is considered.

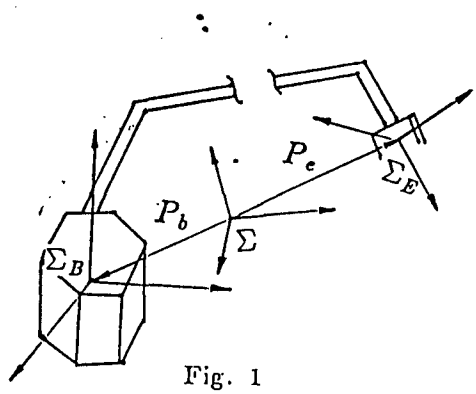

Fig. 1

In comparison with the mass and inertia of the tip hand, those of the robot arm are supposed to be negligible.

Further, no external force is supposed to exert on the sate-lite unit itself but a rotational torque can be generated from GMG, etc., for controlling the satellite attitude.

As the gravitational center of the satellite robot is not varied, the original point of the inertial coordinate system Σ is set at the system mass center and a coordinate system Σ_B is fixed to the sate-lite main unit, that would have its original point at the satellite main unit's mass center and have the satellite inertial main axes as its coordinate axes. Likewise, a coordinate system Σ_E is supposed for the tip hand and ${}^{B}Pe$ as the positional vector at Σ_B of the Σ_E original point and ωb and R_B as the angular vector and rotational transform matrix of Σ_B for Σ.

When $\alpha = (\alpha_1, \alpha_2, \alpha_3)^T$ is set as the Euler angular vector of the satellite main unit and $\omega_b = (\omega_1, \omega_2, \omega_3)^T$, as well as G=(Gij) and Q=(Qij) satisfy $\omega_b = G(\alpha)\dot{\alpha}$ and $\dot{\alpha} = Q(\alpha)\omega_b$, the following results from the kinematics:

$$^{B}P_e = f(\theta) \tag{1}$$

Here, θ is the 6th dimensional rotational angular vector of the robot joints. Time differentiation (denoted $^{B}\frac{d}{dt}$) at Σ_B shows

$$^{B}\frac{d}{dt}(^{B}P_e) = \frac{\partial f}{\partial \theta}\dot{\theta} =: J_{p\theta}\dot{\theta} \tag{2}$$

Likewise, when $^{B}\omega_e$ is supposed to be the angular speed vector of Σ_E for Σ_B, the following is obtained,

$$^{B}\omega_e = J_{\omega\theta}\dot{\theta} \tag{3}$$

$[J_{p\theta}^T \; J_{\omega\theta}^T]^T$ is the Jacobian matrix itself of a ground robot.

As no external force is exerted during operation of the robot arm, the momentum is conserved. Hence,

$$M_b\dot{P}_b + M_e\dot{P}_e = 0 \tag{4}$$

Here, M_b and M_e are masses of the satellite main unit and tip load respectively. P_b and P_e are the positional vectors of the original points of Σ_B and Σ_E in the inertial coordinate system Σ as shown in Fig. 1.

Obviously,

$$P_e = P_b + R_B{}^{B}P_e$$

Hence,

$$\dot{P}_e = \dot{P}_b + \omega_b \times (R_B{}^{B}P_e) + R_B\,{}^{B}\frac{d}{dt}(^{B}P_e). \tag{5}$$

Further, from (2), (4) and (5), the following is established.

$$(M_b + M_e)\dot{P}_b + M_e R_B J_{p\theta}\dot{\theta} + M_e\,\omega_b \times (R_B{}^{B}P_e) = 0 \tag{6}$$

When this is rewritten, the following results.

$$\dot{P}_b = -kR_B J_{p\theta}\dot{\theta} - k[R_B{}^{B}P_e\times]\omega_b \tag{7}$$

Here, the symbol $[\cdot\times]$ means the following equation when an optional 3 dimensional vector $a = [a_x, a_y, a_z]^T$.

$$[a\times] = \begin{bmatrix} 0 & a_z & -a_y \\ -a_z & 0 & a_x \\ a_y & -a_x & 0 \end{bmatrix}$$

Further, $k = \frac{M_e}{M_e+M_b}$ である.

Now, let's think about the system kinetic energy T.

When the rotational matrix of Σ_E for Σ_B is supposed to be $R(\theta)$, the kinetic energy T is a sum of the translation (parallel progress) and rotational energy of the satellite main unit and hand. That is,

$$\begin{aligned} T =& \frac{1}{2}M_b\dot{P}_b^T\dot{P}_b + \frac{1}{2}\omega_b^T R_B I_b R_B^T \omega_b \\ &+ \frac{1}{2}M_e\dot{P}_e^T\dot{P}_e + \frac{1}{2}{}^B\omega_e^T R(\theta) I_e R(\theta)^T {}^B\omega_e \end{aligned} \tag{8}$$

Here I_b and I_e are the inertial tensors of satellite main unit and hand respectively. Using the formulae of (3), (4) and (7), T can be rewritten into the following.

$$T = \frac{1}{2}\dot{q}^T H \dot{q}$$

Here, $\dot{q} = [\omega_b^T, \dot{\theta}^T]^T$ and when $\tilde{q} = [\alpha^T, \theta^T]^T$, H is the function of q. When H is divided into 2 x 2 blocks corresponding to q, the four blocks will be given in the following.

$$\begin{aligned} H_{11} =& R_B[-M_a[{}^BP_e\times]^2 + I_b]R_B^T \\ H_{12} =& -M_a R_B[{}^BP_e\times]J_{p\theta} \\ H_{21} =& M_a J_{p\theta}^T[{}^BP_e\times]R_B^T \\ H_{22} =& M_a J_{p\theta}^T J_{p\theta} + J_{\omega\theta}^T R(\theta) I_e R(\theta)^T J_{\omega\theta} \end{aligned}$$

In the above formulae, $M_a = k^2M_b + (1-k^2)M_e$. Further, a relation formula $[R_B{}^BP_e x] = R_B[{}^BP_e x]R_B^T$ is used. It is obvious that H is a symmetrical regular matrix.

When the Lagrange formula is applied, the robot arm's kinetic formula will be as follows:

$$\sum_{j=1}^{6}(H_{22})_{ij}\ddot{\theta}_j + \sum_{j=1}^{3}(H_{21})_{ij}\dot{\omega}_{bj} + (\tilde{c}_2(\tilde{q}, \dot{q}))_i = \tau_i \tag{9}$$

Here, T_i is the drive torque of a joint i and $\tilde{c}_2(\tilde{q}, \dot{q})$ are the vectors having the following elements.

$$\begin{aligned} (\tilde{c}_2)_i = \sum_{j=1}^{9}\Big[\sum_{k=1}^{3}\frac{\partial(H_{21})_{ik}}{\partial\tilde{q}_j}\omega_{bk} + \sum_{l=1}^{6}\frac{\partial(H_{22})_{il}}{\partial\tilde{q}_j}\dot{\theta}_l\Big]\dot{\tilde{q}}_j \\ - \frac{1}{2}\dot{q}^T\frac{\partial H}{\partial\theta_i}\dot{q} \end{aligned}$$

Here, (H) means the jk element of H.

Then the kinetic formula of the satellite main unit is introduced. The Lagrange formula related to the pseudo coordinate is given in the following manner.[7]

$$\frac{d}{dt}\left(\frac{\partial T}{\partial \omega_i}\right) + \sum_j \sum_k c_{ijk}\omega_k \frac{\partial T}{\partial \omega_j} - \sum_r Q_{ri}\frac{\partial T}{\partial \alpha_r} = \Phi_i \qquad (10)$$

Here,

$$c_{ijk} = \sum_s \sum_r \left(\frac{\partial G_{jr}}{\partial \alpha_s} - \frac{\partial G_{js}}{\partial \alpha_r}\right) Q_{sk} Q_{ri}$$

Summarizing the (9) and (10), the following kinetic formulae are obtained.

$$H_{11}(\bar{q})\dot{\omega}_b(t) + H_{12}(\bar{q})\ddot{\theta}(t) + \bar{c}_1(\bar{q}, \dot{q}) = \Phi \qquad (11)$$

$$H_{21}(\bar{q})\dot{\omega}_b(t) + H_{22}(\bar{q})\ddot{\theta}(t) + \bar{c}_2(\bar{q}, \dot{q}) = \tau \qquad (12)$$

Here, cl is a vector having the following element.

$$(\bar{c}_1)_i = \sum_j \sum_k c_{ijk}\omega_k \frac{\partial T}{\partial \omega_j} - \sum_r Q_{ri}\frac{\partial T}{\partial \alpha_r} + \left([\dot{H}_{11} \quad \dot{H}_{12}]\dot{q}\right)_i$$

Further, $\Phi = (\Phi_1, \Phi_2, \Phi_3)^T$, $\tau = (\tau_1, \cdots, \tau_6)^T$ are respectively control torques of the satellite attitude and robot joints.

3. Grasping Rotational Objects

In this section, we will describe a control algorithm in grasping an object rotating in a complicated manner with a robot arm. An object with its symmetrical axis is supposed to be in a tumbling movement without external force nor torque as shown in Fig. 2.[3]

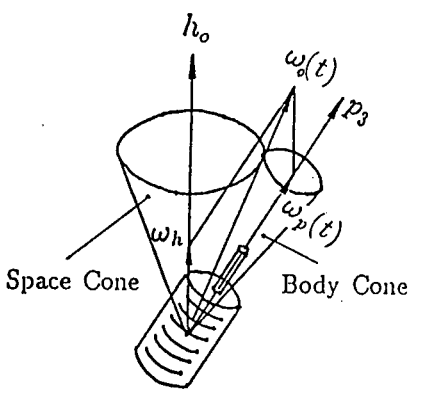

Fig. 2

It is also supposed that the angluar momentum vector h_o and the longest main axis direction vector p3 of the object and the angular velocity vector $\omega_o(t)$ are always on a similar plane. The body cone rotates in contact with the space cone.

The projections of $\omega_o(t)$ to h_o and p3 are written as $\omega_h(t)$ and $\omega_p(t)$. As h_o is constant, it is detected first and shifted so that the mass center of the

satellite robot system comes on the h_o axis with the robot arm folded on the satellite main unit. Then, with no external force applied, the mass center of the satellite robot system at that time is set as the inertial coordinate system. When the robot is moved, the angular velocity and central position of the satellite main unit are also varied concurrently, but it is vital to give a satellite torque and a robot's joint torque so that the satellite main unit's angular velocity $\omega_b(t)$ agrees with ω_h and the robot hand's angular velocity agrees with $\omega_p(t)$ respectively. The control rule for that purpose is shown below.

Fig. 3 shows its conceptual operation diagram.

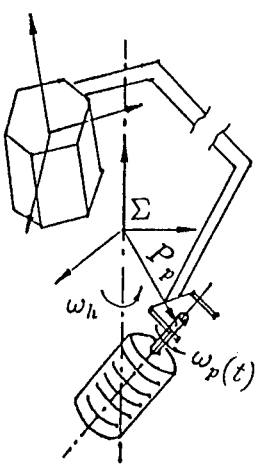

Fig. 3

The tip velocity of a robot arm in the inertial coordinate system is given in the following from the (5) and (7) formulae.

$$\dot{P}_e = (1-k)[R_B\, {}^B P_e \times]\omega_b + (1-k)R_B J_{p\theta}\dot{\theta}$$

And, the angular velocity is given.

$$\omega_e = \omega_b + R_B\, {}^B\omega_e = \omega_b + R_B J_{\omega\theta}\dot{\theta}$$

When $\dot{e} = (\dot{P}_e^T,\ \omega_e^T)^T$, it is understood the following is satisfied.

$$\dot{e} = J_\Omega \omega_b + J_\theta \dot{\theta}$$

Here, JΩ and Jθ are given in the following formulae.

$$J_\Omega = \begin{pmatrix} (1-k)R_B[{}^B P_e \times]R_B^T \\ I \end{pmatrix},\quad J_\theta = \begin{pmatrix} (1-k)R_B J_{p\theta} \\ R_B J_{\omega\theta} \end{pmatrix}$$

Then, $\dot{e}_p = [\dot{P}_p^T,\ \omega_p^T]^T$ is supposed to be a combined vector of the velocity and angular velocity at Σ of the object and ε be a vector with the position ${}^E P_p$ and attitude angle ${}^E\beta_p$ (Roll, Pitch, Yaw) combined. That is $\varepsilon = [{}^E P_p^T,\ {}^E\beta_p^T]^T$.

This can be measured if a camera is set to the hand. The purpose of control is to bring this ε to a proximity of 0 and grasp the object. The control rule for that purpose is introduced in the following manner.

The Lyapunov function for optional regular symmetry constant matrixes W and Kp are chosen as follows:

$$V(t) = \frac{1}{2}[(\omega_b - \omega_h)^T, (\dot{\theta} - J_\theta^{-1}(\dot{x}_p - J_\Omega \omega_b))^T]W \cdot \begin{pmatrix} \omega_b - \omega_h, \\ \dot{\theta} - J_\theta^{-1}(\dot{x}_0 - J_\Omega \omega_b) \end{pmatrix} + \frac{1}{2}\varepsilon^T K_p \varepsilon \tag{13}$$

Here, Jθ is supposed to be always regular.

By differentiating both sides of V(t) with time and using the dynamic equations of (11) and (12), the control input is determined as follows:

$$\begin{pmatrix} \Phi \\ \tau \end{pmatrix} = \begin{pmatrix} \tilde{c}_1 \\ \tilde{c}_2 \end{pmatrix} - HE^{-1} \begin{pmatrix} -\dot{\omega}_h \\ f(t) \end{pmatrix} - HE^{-1}W^{-1}\left\{ K \begin{pmatrix} \omega_b - \omega_h \\ \Delta\dot{\theta} \end{pmatrix} + \begin{pmatrix} 0 \\ J_\theta^T \Lambda^T K_p \varepsilon \end{pmatrix} \right\} \tag{14}$$

Then, it is known V(t) is non-positive. That is,

$$\dot{V}(t) = -(\omega_b - \omega_h)^T K_\omega (\omega_b - \omega_h) - \Delta\dot{\theta}^T K_v \Delta\dot{\theta} \leq 0 \tag{15}$$

However, in the formulae (14) and (15), the following is satisfied.

$$f(t) = -J_\theta^{-1}(\ddot{x}_p - \dot{J}_\Omega \omega_b) - \dot{J}_\theta^{-1}(\dot{x}_p - J_\Omega \omega_b),$$
$$\Delta\dot{\theta} = \dot{\theta} - J_\theta^{-1}(\dot{x}_p - J_\Omega \omega_b)$$

And, E is the following matrix.

$$E = \begin{pmatrix} I & 0 \\ J_\theta^{-1} J_\Omega & I \end{pmatrix}$$

Obviously, an inverse matrix E^{-1} does exist. Kω and Kv are optional symmetrical regular constant matrixes with K = block diag {Kω,Kv}. Further, Λ is set as follows:

$$\Lambda = -\text{ block diag } \{I,\ F^{-1}({}^E\beta_p)\}$$

Here, $F({}^E\beta_p)$ is a 3 x 3 transform matrix satisfying $F({}^E\beta_p)\,{}^E\omega_p = F({}^E\beta_p)\,{}^E\dot{\beta}_p$. Eωp denotes an angular velocity of the object as seen in the hand coordinate system. It can be confirmed that F is regular in the proximity of ${}^E\beta_p = 0$. When the object is axially symmetric, ω is constant, that is, $\omega_h = 0$.

Then, let us check when V(t) is 0. In such a case, from the equation (15), the following is satisfied.

$$\omega_b = \omega_h, \qquad \dot{\theta} = J_\theta^{-1}(\dot{e}_p - J_\Omega \omega_b) \tag{16}$$

When the error vector of position and attitude ε is supposed to be not 0, it is known that $[0, J_\theta^T \Lambda^T K_p \varepsilon]^T = 0$ by substituting the control torque formula (14) for the kinetic formulae (11) and (12) and taking (16) into account. This means $\varepsilon = 0$. Therefore, the closed loop has an asymptotic stability from the LaSalle theorem. Now, it should be noted that either of x_p or x_p in the (14) formula is an expression of the inertial coordinate system. From Fig. 1, the following is established.

$$P_p = P_b + R_B {}^B P_p \tag{17}$$

And, the ${}^B P_p$ is the positional vector of the object as viewed from the satellite main unit. By differentiating both sides of the formula (17) with time and using the formula (7), the following is obtained.

$$\begin{aligned} \dot{P}_p = &- k R_B J_{p\theta} \dot{\theta} - k[R_B {}^B P_e \times]\omega_b \\ &+ [R_B {}^B P_p \times]\omega_b + R_B {}^B \dot{P}_p \end{aligned} \tag{18}$$

In regard to ω_o, the following equation is established.

$$\omega_o(t) = \omega_b + R_B {}^B \omega_o(t) \tag{19}$$

In this article, it is assumed that it is possible to measure by any means the attitude angle α and angular velocity $\omega_b(t)$ of the satellite itself, as well as the position ${}^B P_p$, velocity ${}^B P_p$ and angular velocity ${}^B \omega_o(t)$ of the object from the coordinate Σ_B. Therefore, $\omega_o(t)$ is given in the formula (19) and $\omega_p(t)$ can be calculated from $\omega_p = \omega_o - \omega_h$ as shown in Fig. 2 and can be obtained from the formula (18).

Further, it is assumed that x_p can be obtained from a difference of x_p. Hence, the control rule of the formula (14) can be realized. In summary of the foregoing, the physical quantities to be measured and calculated are as follows:

(1) To detect angular momentum vector h_o of the object.
(2) To measure attitude angle (Euler angle) α and angular velocity ω_b of the satellite main unit.
(3) To measure rotational angular velocity $\omega_o(t)$ of the object {ω_h and $\omega_p(t)$ are known from its result}.
(4) To measure position $\theta(t)$ and velocity $\dot{\theta}(t)$ of each joint of the robot.
(5) To measure position ${}^B P_p$ and velocity ${}^B P_p$ of the object as viewed from the satellite main unit.

(6) To measure the position and attitude ε of a target from the robot hand coordinate system Σ_E.
(7) To calculate quantity $\dot{x}_p$ in the inertial coordinate system using the formula (18).
(8) To calculate ${}^B\dot{x}_p$ from ${}^B\ddot{x}_p$ using numerical differentiation.

4. Conclusion

We introduced here the dynamic kinetic formula of a space robot and proposed a control rule to grasp a complicated rotational body with the robot hand. It is possible to calculate the control torque by measuring the physical quantities such as positions, attitudes and velocities of the robot hand and grasping object as viewed from the satellite main unit, as well as the attitude angle, etc. of the satellite itself.

References

[1] R. W. Longman, R. E. Lindberg and M. F. Zedd, "Satellite-mounted robot manipulators-new kinematics and reaction moment compensation", Int. J. Robotics Research, Vol 6, No 3, pp 87-103, 1987.

[2] Y. Umetani and K. Yoshida, "Resolved motion rate control of space manipulators with generalized Jacobian matrix," IEEE Trans. Robotics and Auto., Vol 5, No 3, pp 303-314, 1989.

[3] M. H. Kaplan, Modern Spacecraft Dynamics & Control, John Wiley & Sons, 1976.

[4] Masuya, Miyazaki and Arimoto, "Sensor Feedback Control of a Space Manipulator", 5th Japan Robotics Society Symposium, pp 245-248, 1987.

[5] Tsuchiya and Yamada, "Space Robot (Dynamics and Control of a Space Manipulator System", Japan Machinery Society 67th Symposium Paper, pp 53-60, 1988.

[6] Yamada and Tsuchiya, "Kinetic Control of a Space Manipulator Suppressing Change of the Satellite Main Body", SAIRAS, pp 27-30, 1988.

[7] Goto, "Dynamics Theory", Scholastic Press, 1983.

Configuration of Manipulator Control System for Space Robots

906C0047 Tokyo SAIRAS 89 PROCEEDINGS in Japanese 18-19 Oct 89 pp 184-187

[Article by Kenji Ogimoto, Osamu Miki, Osamu Noro, Kiyoshi Ioi and Nobuyoshi Muroi of Kawasaki Heavy Industries Ltd.]

[Text] Abstract

In the near future, it is expected that the space robots will perform the dexterous and complicated tasks required in the space activity, such as truss assembly, ORU change out, retrieval of debris, etc. In order to perform these tasks, the manipulator control systems should have the ability to realize the motions composing the tasks. They are positioning, force generation, compliant motion, position/force hybrid motion, and so on. As the functions required to the control systems to realize these motions, following control criteria are chosen.

(a) Load adaptive control

In the space, due to the small gravity, the range of the mass of the loads handled by the manipulators is wider than that on the earth; accordingly, the response of the manipulators varies widely influencing the performance of the robot. The control parameters should be changed according to the loads.

(b) Disturbance compensation control

The base of the manipulators is not necessarily combined rigidly with the objects. So the external forces on the robots, or on the objects easily cause the relative motion between the robots and the objects which can be compensated by the relative position/velocity feedback.

(c) Impedance control

The purpose of the impedance control is to respond properly to the reaction force from the objects, when mating connectors, capturing the objects, or so, in order to avoid the overload on the contact point and to follow the movement of the object.

(d) Position/force hybrid control

In many tasks, it is required to control position to some directions and to control force to other directions simultaneously. The examples are, mating connectors, fastening bolts, cleaning, etc.

Most of the tasks are carried out by the combination of these controls. For example, when capturing the flying object, positioning control is done first before the manipulator touches the object. Next, impedance control with low stiffness is done to absorb the impact, followed by the tuning of the control parameters according to the load adaptation algorithm.

The important thing is to carry out those functions at a time. This report presents the configuration of the control system which realizes above 4 functions in cooperation with each other.

1. Introduction

Tasks required of robots in space are diversified - among them - replacement of instruments, maintenance and check, assembly of structures, but basically these works have to be performed by a single robot.

In this paper, we will concentrate on the control technology of a manipulator most operative among space robots and describe what control functions are required and how the control system should be structured.

2. Conceptual Diagram of a Space Work Manipulator Control System

The manipulator control system configuration can be roughly categorized into the following three sections as shown in Fig. 1.

- o Section for planning of space works
- o Section of deploying the arm in specific movement
- o Section for executing each operation

It is reasonable to think several hands are required in space works and we will discuss here a control system configuration to execute each operation of each arm.

3. Required Control Functions

Control functions deemed important in executing each operation at will are shown below.

(a) Load adaptive control

In handling objects with various weights in space, the control parameters must be changed corresponding to each load so as not to vary the response characteristics but the load characteristics are seldom known in advance.

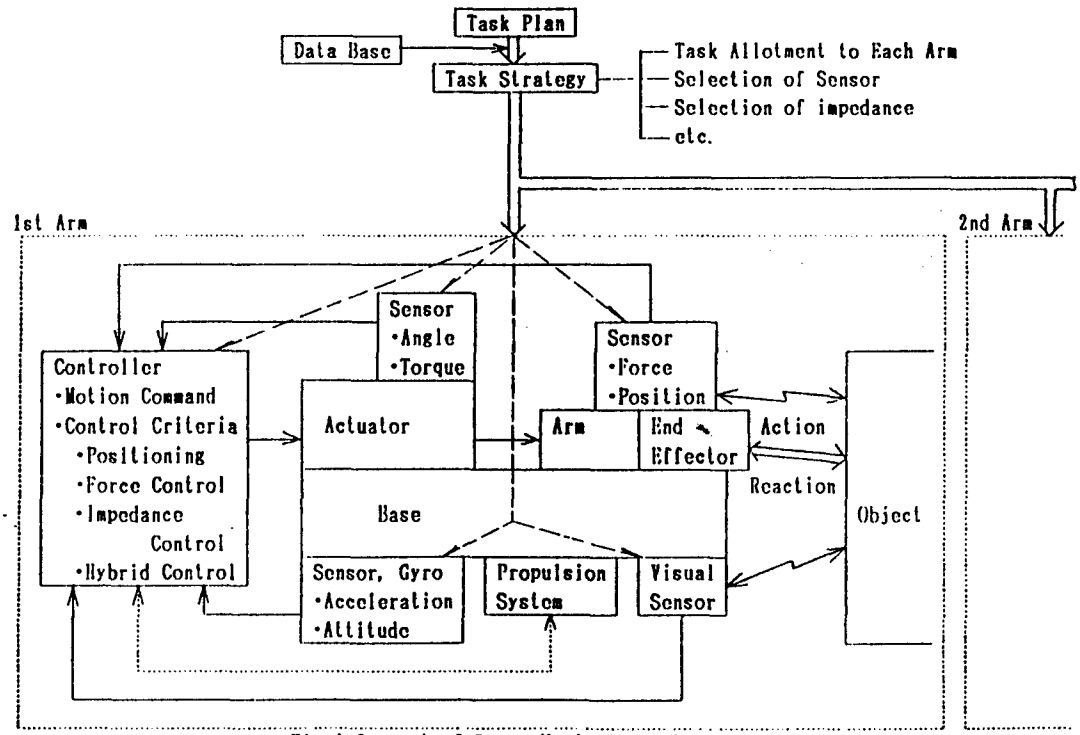

Fig. 1 Concept of Space Manipulator Control System

Therefore, it is generally conceived to move a robot and identify its load from the response.(1)

(b) Disturbance compensation control

In space works, the robot itself and work objects are often loosely connected and any external force might remove the objects from the robot, affecting the space works. To avoid such a mishap, a method is provided to detect a relative movement of the robot and objects, thereby correcting commands to the robot and cancelling its movement due to disturbances.

(c) Impedance control

When the robot hand gets a reaction force from the work objects, it is conceived to give a proper response to such a reaction force and it is called the impedance control. In space works, connectors may be misaligned and an impact may be generated in grasping a flying object and these misalignment and impact are absorbed or lessened with the impedance control.

(d) Position/force hybrid control

In many works, it often happens that the position in a direction must be controlled while the force in another direction should be controlled. In space works, these controls are often needed in the following.

o Aligning connectors

o Tightening bolts

o Cleaning

They are shown in Fig. 2 and functions mentioned in the above (a) to (d) are diagrammed in Fig. 3.

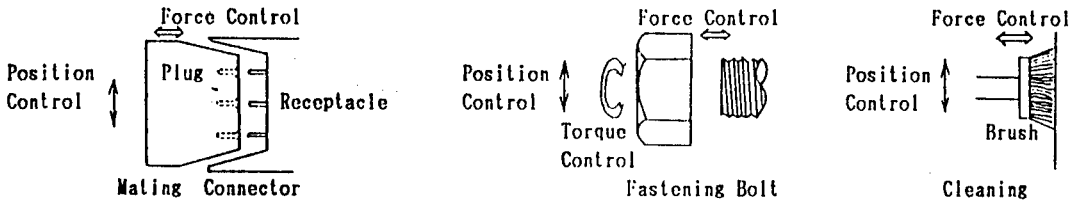

Fig. 2 Examples of Position/Force Hybrid Control

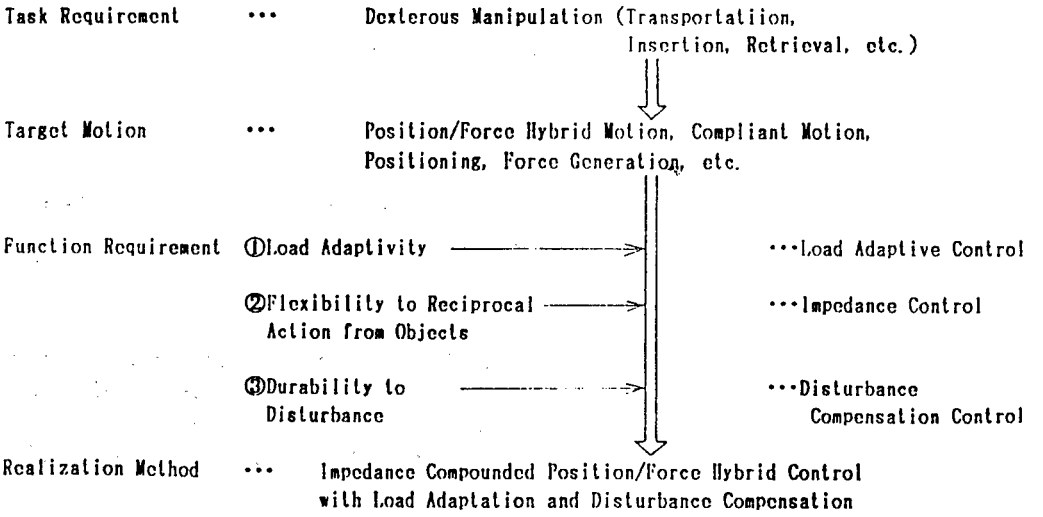

Fig. 3 Function Diagram of Space Manipulator Control System

4, Configuration of the Control System

First, the impedance control and the position force hybrid control are compounded. It is impossible to control the position and force to any value simultaneously. Therefore, in the position control space, a normal impedance control is used and, in the force control space, force is taken as the control quantity to form as an impedance control space without controlling the position.(2)

In a space compounding the position control and impedance control, the required response is as follows:

$$M_d S\ddot{y} + D_d S(\dot{y}-\dot{y}_d) + K_d S(y-y_d) = SF \qquad (1)$$

In a space compounding the force control and impedance control, the required response can be written as follows:

$$M_d(E-S)\ddot{y} + D_d(E-S)(\dot{y}-\dot{y}_d) = (E-S)(F-F_d) \qquad (2)$$

Here,

Md : Required mass

Kd : Required spring constant

Dd : Required damping

S : Space switching matrix

y : Arm position

yd : Arm target position

F : External force on arm end

Fd : Target force on arm end

E : Unit matrix

When this formulae (1) and (2) are compounded (added), the following is established.

$$M_d\ddot{y} + D_d(\dot{y}-\dot{y}_d) + K_d S(y-y_d) = F-(E-S)F_d \qquad (3)$$

This formula (3) is the target response of arm end.

In the meanwhile, when it is supposed no static force is exerted, the robot arm movement can be described in the following formula.

$$M\ddot{y} + h = {}^tJ^{-1}\tau + F \qquad (4)$$

Here,

M : Generalized inertial matrix

τ : Joint torque

h : Non-linear term of velocity

J : Jacobian matrix

The required joint torque is obtained in the following by deleting y from the formulae (3) and (4).

$$\tau = {}^tJ(MM_d^{-1}(K_d S(y_d-y) + D_d(\dot{y}_d-\dot{y})) + (MM_d^{-1}-E)F - MM_d^{-1}(E-S)F_d + h) \qquad (5)$$

To this, by adding the parameter adjustment mechanism for fluctuations of relative position with the object, velocity loop and load for correcting disturbances, a control system satisfying the above (a) to (d) simultaneously is conceivable. Its block diagram is shown in Fig. 4.

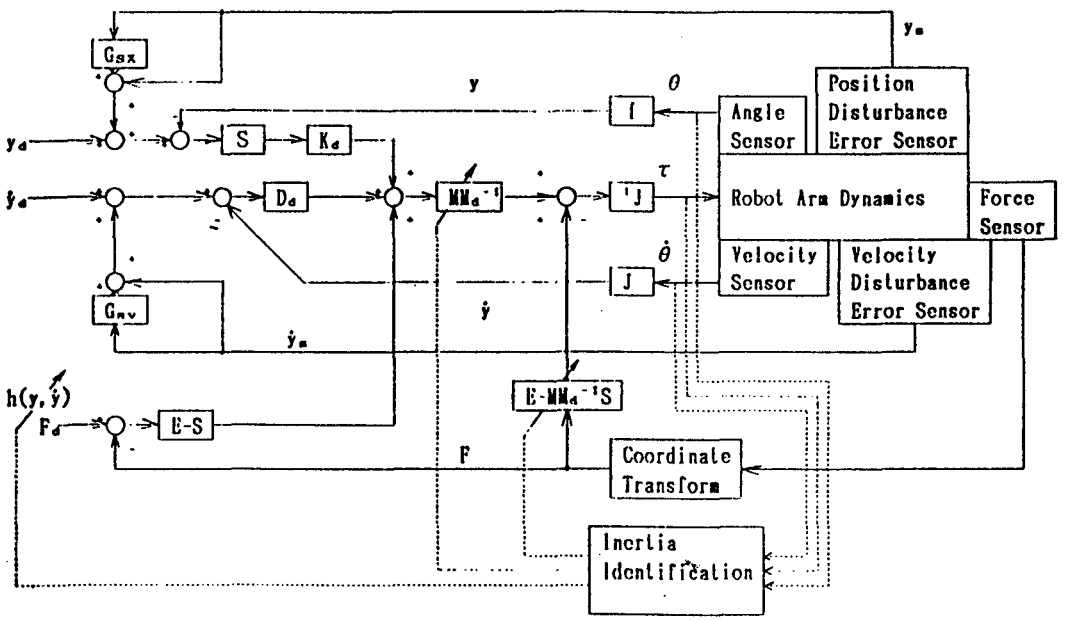

S :Switchig Matrix
J :Jacobian Matrix of Robot Arm
h :Nonlinear Term of Velocity
θ :Angular Displacement
y :Position of Arm in Work Coordinate
$\dot{y}$:Velocity of Arm in Work Coordinate
F :External Force on Arm End
y_e:Position Error in Work Coordinate
G_{sx}:Position Error Compensator
K_d:Target Stiffness of Arm End(3x3Matrix)
M_d:Target Mass of Arm End(3x3Matrix)

E :Unit Matrix
f :Direct Kinematics of Robot Arm
τ :Torque Command
$\dot{\theta}$:Angular Velocity of Robot Arm
y_d:Target Position of Arm End
$\dot{y}_d$:Target Velocity of Arm End
F_d:Target Force on Arm End
$\dot{y}_e$:Velocity Error in Work Coordinate
G_{sv}:Velocity Error Compensator
D_d:Target Damping of Arm End(3x3Matrix)

Fig. 4 Block Diagram of Impedance Compounded Position/Force Hybrid Control System with Load Adaptation and Disturbance Compensation

5. Conclusion

We showed in block diagrams functions and their configurations required in the manipulator control system of a space robot. What we suggested here is how to structure an entire control system and it requires specific discussions separately how to implement each control element.

Part of this study has been commissioned by the National Space Development Agency of Japan.

References

(1) Kouichi Maeda, "Dynamic Model of a Robot Arm and its Identification", Japan Robotics Society Journal Vol 7, No 2, 1989.

(2) R.J. Anderson and M. W. Spong: "Hybrid Impedance Control of Robotic Manipulators", IEEE Journal of Robotic and Automation, Vol 4, No 5, 1988.

Development of Target Capturing Device With Flexible Capability

906C0047C Tokyo SAIRAS 89 PROCEEDINGS in Japanese 18-19 Oct 89 pp 198-201

[Article by Yoshitugu Toda, Kazuo Machida, Toshiaki Iwata, Shoichi Iikura, Tadashi Komatu, Masaru Oka and Toshio Honda of Electrotechnical Laboratory, Toshiba Corporation]

[Text] Abstract

A smart end effector that is attached at the tip of a large arm or on a free flying teleoperator to capture a drifting target object in space is developed. The mechanism consists of three linear actuators for positioning and three-dimensional gimbals mechanism for orientation. As the reduce of the problem originated by the uncertainty of the positioning of the large arm or the free-flying teleoperator was aimed at, this mechanism was chosen because of its compactness, controllability and the movement equality. The linear actuator consists of a DC brushless motor with a ball-screw driver that has good controllability and high stiffness. As this mechanism is unstable, three parallel mechanisms each of that consists of a spline and some bevel gears are attached to keep the platform of the gimbals parallel to the basement of the end effector. An approach and distance sensor enables the sensor-feed-back to a target marker. As it is rather easy to solve forward and inverse kinematics, the cycle time is shorter than 16mS which is the time interval to take in the position data of the target object from the approach and distance sensor. Some preliminary experiments to trace a target marker showed the good controllability. The qualification test shall be undertaken on a 2-Dimensional test bed that consists of a flat bed and an air bearing system which enables frictionless condition to simulate micro-gravity condition.

1. Introduction

The robotics technology is a must in the space development and a safe and rational new horizon can be exploited by relying on this technology in environment unfavorable to human in terms of vacuum and radio activity. In such an instance, a large crane-type manipulator arm or free-flying teleoperator is used in space operation and the relative velocity between a captor side and captive side drifting in the weightless condition of space should be held to the minimum.

A large arm and teleoperator do not necessarily have the optimum positioning control method for the tip of an end effector and it is not so easy to keep the relative position for the target. To solve this problem, compensation must be made with a degree of freedom as much as required by the end effector unit and local sensor feedback control loop. From this viewpoint, we have developed a target capturing device with flexible and adaptive capability and the following is our report on this development.

2. Mechanism

For the purpose of our study this time, we though it better for the mechanism unit to have a high rigidity and compact shape with few singular points in case of the inverse kinematics.

When it is controlled with a software servo, it is optimal to have topology allowing required position and velocity easily in a short operation time. From these requirements, we have adopted a mechanism of 3-axis parallel + 3-axis gimbals. However, we used a neck swing (oscillator) with one degree of freedom this time instead of gimbals as we are going to experiment mainly on a 2-dimensional test bed.

The 3-axis parallel has no singular point in the operation range allowing it to obtain forward and inverse kinematics easily but is instable in structure and needs to incorporate a correction device somehow. For this, we used a combination of bevel gears and spline. Each axis of the parallel is a linear actuator activated by a DC brushless motor with a ball screw driver and it satisfies both high controllability and rigidity. Fig. 1 shows a photo of the end effector installed on the experimental 2-dimensional test bed.

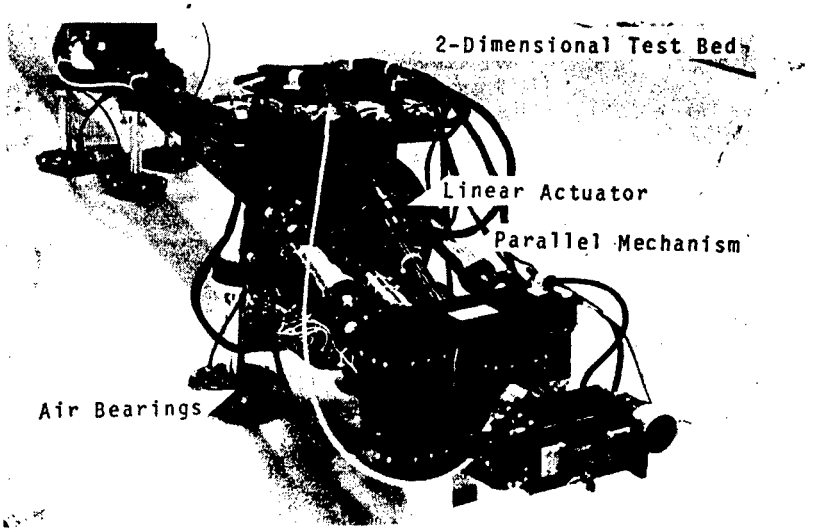

Figure 1. The End Effector on 2-Dimensional Test Bed

3. System Configuration

Fig. 2 shows a block diagram of the entire system. There are two CPUs each for the host side and control side. The host CPU is responsible for the man-machine interface mainly analyzing commands and processing data. For this purpose, we used a lap-top personal computer with Intel 80286. The control side CPU mainly controls the end effector servo and to a lessor degree retrieves data. For this purpose, a lap-top personal computer with Intel 80386 is used as high processing is needed. Regarding the sensors for sensor feedback, an approach and distance sensor and force/torque sensor could be used, but at present only the first one is used. This sensor as reported earlier is capable of outputting the relative position and direction in video cycle to the target shown in Fig. 3.

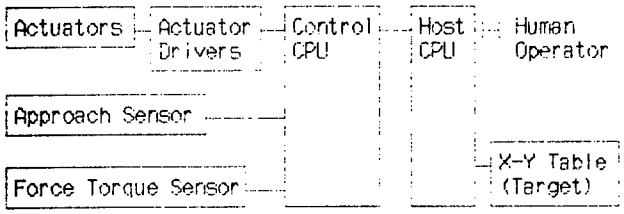

Figure 2. System Block Diagram

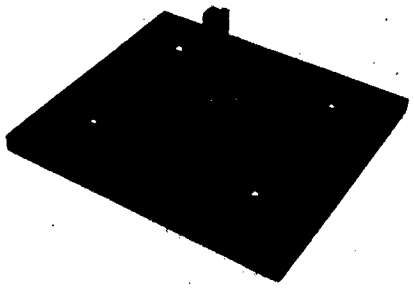

Figure 3. Target Marker

A force/torque sensor with 6-axis output has already been incorporated and its software is now being implemented.

4. Outline of Software

The control cycle for the end effector has been matched with an output cycle of the approach and distance sensor, that is, 1/60 seconds. Commands are input from the host side keyboard and transferred to the controller side. The commands are basically classified into position controls, tracking controls and others, but an interpreter language combining them can also be used. This language is used in setting preliminary variables and for condition identification formulae, etc.

A list of commands is shown in Table 1 and specifications of the interpreter language is in Table 2.

5. Results of the Experiment

Fig. 4 shows an example of the captor output in tracking a reciprocating target. There is a slight delay, but it is assumed this can be corrected by adding a compensation element to the target velocity. Further, we have

Table 1. Command List

item	operatrion
ad	Drive an actuator directly
bc	Activate a brake of an actuator
bo	Release a brake of an actuator
ps	Move to an orderd position
t4	Track a target with 4-Dimensional senser-feed back control (x, y, z, θ_x)
t3	Track a target with 3-Dimensional senser-feed back control (x, y, θ_x)
sl	Servo-lock whole actuators
bl	Brake-lock whole actuators
br	Brake-release whole actuators
gc	Close a gripper
go	Open a gripper
ge	Free a gripper
sb	Execute a submit file (Invoke the Interpreter)
ss	Dispaly and/or store senser data
up	Update a parameter table
sp	Set a maximum speed of the end effector
rs	Reset the end effector

Table 2. Specification of the Interpreter

Command line	Executable whole command in Table 1.
Variables	Integer, 50 variables maximum
	Definition: $<name>
	Executable Operatations: addition substitution
Directives	VAR <variable> Define a variable
	GOTO <lable> Go to <label>
	IF ... ELSE ... ENDIF Conditional execution
	WHILE ... BREAK END Loop
	PAUSE Keep current state
	EXIT Exit from the Interpreter mode

made an experiment of capturing the target in circle orbit using the interpreter language, which can be put to reasonable practice. At present, an experiment is being prepared to capture a free target with the language provided on the tip of an arm, simulating a large manipulator arm on the 2-dimensional test bed.

6. Conclusion

This device has just been completed and its capability will be ascertained by setting various parameters from now on. Further, we are considering to make the movement smoother after capturing the target, by conducting a feedback control with a force/torque sensor and verifying the possibility and supremacy of the active compliance control.

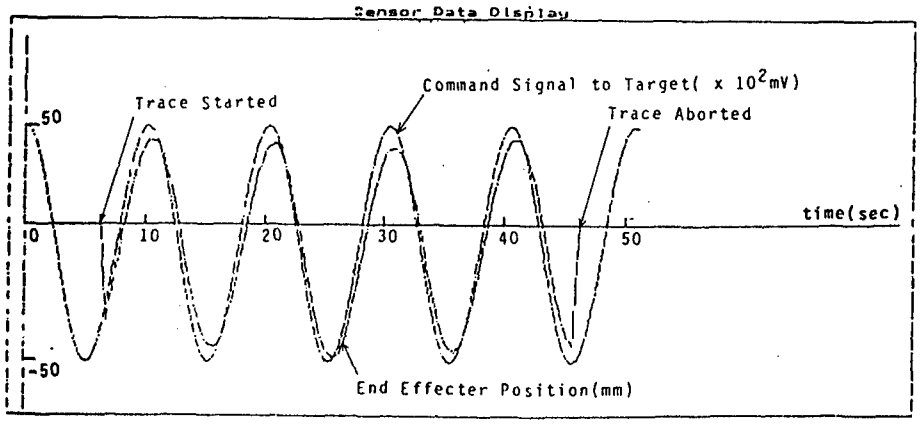

Figure 4. Experiment Results of 3-Dimensional Tracking

Capture of Free-Flying Target Using Visual Information

906C0047 Tokyo SAIRAS 89 PROCEEDINGS in Japanese 18-19 Oct 89 pp 206-209

[Article by H. Shimoji, M. Inoue and K. Tsuchiya from Mitsubishi Electric Corporation together with K. Ninomiya, I. Naktani and J. Kawaguchi from the Institute of Space and Astronautical Science]

[Text] Abstract

This paper shows a recognition algorithm of a moving target using visual sensors, a manipulator control algorithm using recognized data, and capture experiments based on these algorithm.

In order to develop an autonomous space robot, we constructed the ground simulation system where relative motion between the space robot and the target in zero gravity environment is simulated by combining a computer simulation and 6 axis servo mechanism. As operating this system, experiments of autonomous capture of the target are performed.

As 4 infrared light emitting diode (LED) are attached on the target and the image is taken in by 2 CCD cameras through infrared-through filter, light points are easily extracted. From the information of LED points, the target position and attitude are calculated by the use of extended Kalman filter including the equation of motion of the target. This filter estimates 12 states; position, attitude, linear velocity, and angular velocity. As this filter has redundancy in the observation, it can be adapted to the case that some points are occluded. In order to correct the estimation errors due to the misalignment, a LED is attached to the hand and the hand position is calculated by the visual sensors and by joint encoders. These calculation cycle is about 450-500[msec]. The manipulator is about 1[m] long and it has 8 joints including the end effector. The trajectory is generated so as that the hand approaches the target in a straight line from the present position. With respect to the attitude, the attitude of hand approaches that of the target at the constant rate. The trajectory is corrected every time when the states of the filter are updated.

Based on these algorithm, we perform autonomous capture experiments of the target which moves in 6 D.O.F. under the condition that the relative motion between the target and the space robot in zero gravity space is

simulated. As a result, it is confirmed that the space robot can catch the target automatically even if they are floating in zero gravity environment.

1. Introduction

We are developing a self-regulating mobile robot shown in Fig. 1. For this purpose, we have developed a simulator device (Fig. 2), simulating a relative movement in weightless space as a tool. By activating this device and simulating a weightless space, we have experimented a capturing of a target satellite (TS) with a slow motion of 6 degree freedom using video information only. The following is a description of the TS recognition algorithm and the manipulator control method used in this experiment.

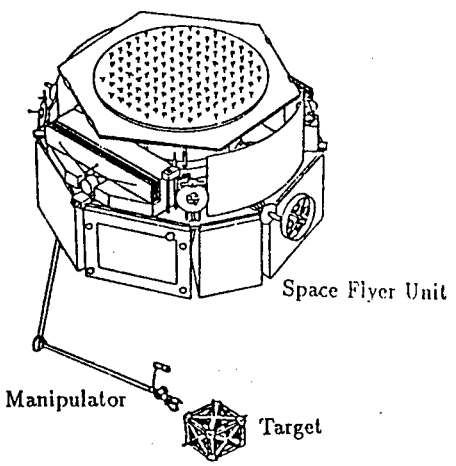

Fig.1. Space Robot

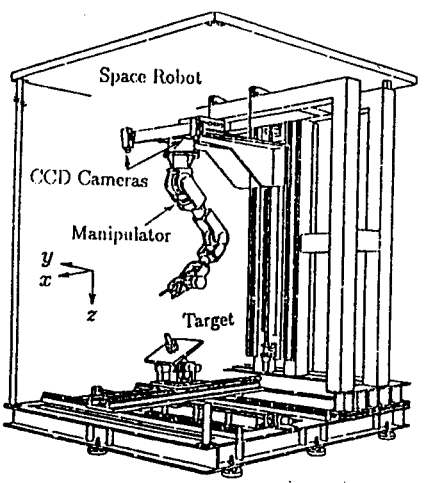

Fig.2. Outlook of the Simulation System

2. TS Recognition Using Visual Information

Based on the TS recognition using an extended Kalman filter (EKF), we have achieved a recognition with practical accuracy level by correcting the filter output through detecting the position of the manipulator from video images.

2.1 Structure of the visual system

The visual system has a structure as shown in Fig. 3.

An infrared light emitting diode (IRLED) is attached each one on the four TS faces, its light point is easily picked up by inputting it through the infrared-through filter of two CCD cameras. The image recognition processing is made using this light point information only.

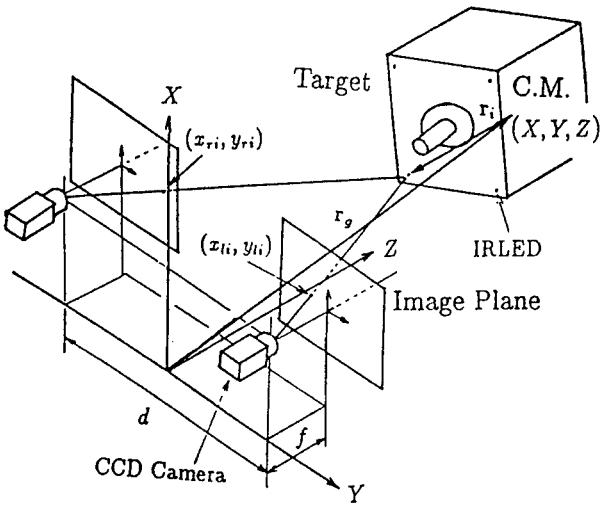

Fig.3. Image Coordinate System

2,2 Recognition using EKF

To recognize TS from visual information, we adopted an EKF. The EKF does not include TS dynamics, although it does include dynamics of the robot itself, errors are generated from a manipulator movement which are caused in the satellite movement. However, these errors are modified by processing images at a high speed,

The status vector estimated by EKF is as follows;

$$\mathbf{x} = [\mathbf{r}_g^v, \mathbf{p}, \dot{\mathbf{r}}_g^v, \dot{\mathbf{p}}]^T \tag{1}$$

Here, $\mathbf{r}_g^v$ and P is respectively a set of the TS's gravitational position vector and Euler angle as viewed from the visual coordinate system. The $\cdot$ denotes a time differentiation. The observation vector is assumed as follows:

$$\mathbf{z} = [\cdots, x_{li}, y_{li}, \cdots, x_{rj}, y_{rj}, \cdots]^T \tag{2}$$

Here, the (x_{li}, y_{li}) and (x_{rj}, y_{rj}) are respectively the light point coordinate picked up from the left and right cameras, Usually, four IRLED images are picked up and 16 of z elements are available but they are increased or decreased depending on appearance or disappearance of the light points.

A dynamics model of TS has a translation (parallel progress:isokinetic linear) motion and rotation (nutation) motion. That is, the following is satisfied.

$$\begin{cases} \mathbf{r}_{g,k+1}^v = \mathbf{r}_{g,k}^v + \dot{\mathbf{r}}_{g,k}^v \cdot \Delta t, & \dot{\mathbf{r}}_{g,k+1}^v = \dot{\mathbf{r}}_{g,k}^v \\ \mathbf{p}_{k+1} = \mathbf{p}_k + \dot{\mathbf{p}}_{k+1} \cdot \Delta t, & \dot{\mathbf{p}}_{k+1} = \mathrm{func}(\mathbf{p}_k, \dot{\mathbf{p}}_k) \end{cases} \tag{3}$$

Here, Δt is a calculation cycle time of the filter and the affix k is a time quantatized with Δt and the func() is a non-linear function including calculation of the Euler formula. Summing them up, the following is expressed.

$$x_{k+1} = f(x_k) \tag{4}$$

Then, in regards to observation, the Z_k which is a set of light point coordinates in the images can be expressed in the following using a non-linear function h regarding X_k.

$$z_k = h(x_k) \tag{5}$$

From the above, the EKF is structured in the following manner.

$$\begin{cases} \tilde{x}_{k+1} = f(\hat{x}_k) \\ \hat{x}_k = \tilde{x}_k + K_k\{z_k - h(\tilde{x}_k)\} \end{cases} \tag{6}$$

$$\begin{cases} \mathbf{K}_k = \mathbf{P}_k \mathbf{H}_k^T \mathbf{W}^{-1}, \mathrm{P}_k = (\mathrm{M}_k^{-1} + \mathrm{H}_k^T \mathbf{W}^{-1} \mathbf{H}_k)^{-1} \\ \mathbf{M}_k = \mathbf{F}\mathbf{P}_{k-1}\mathbf{F}^T + \mathbf{U}, \ \mathbf{F} = [\frac{\partial f}{\partial x}], \ \mathbf{H} = [\frac{\partial h}{\partial x}] \end{cases}$$

Here, the $\tilde{X}_k$ is a predicted value of $\hat{X}_k$ and X_k is an estimated value of X_k. The U and W are error covariances of observation and dynamics respectively, and the following is satisfied when u and v are constants.

$$\mathbf{W} = w \cdot \mathrm{I}_{16\times16}, \quad \mathrm{U} = u \cdot \mathrm{I}_{12\times12}$$

In actual calculation, the calculation quantity is comparatively little as F_k, U, W and H_k are often 0. Depending on the number of light points, the calculation cycle time was about 450 to 500 msec (including the processing in 2.3) using the MC68020/68881 (16 MHz).

2.3 Correction using a light source at the hand tip

Estimation using the EKF is unable to correct errors in manufacturing and initial settings fully. So, we have tried to minimize errors of the position which cause troubles in capturing the target by attaching a light emitting diode at the hand tip. As shown in Fig. 4, a position error of e is generated in the hand when an error e exists between the original point O_m of the manipulator coordinate system and the original point O_v of the image coordinate system and the control command value is set at the following using the hand position vector r_h^m calculated from a joint angle of the manipulator.

$$r_t^m = r_h^m \tag{7}$$

Therefore, r_h^v is obtained using the LED on the hand tip and the error e is corrected using the following command value.

$$r_t^m = r_t^v + e = r_t^v + (r_h^m - r_h^v) \tag{8}$$

In the formula (8), the attitude error between the two coordinate systems is disregarded. This much of an attitude error does not pose an obstacle in capturing the TS. In Fig. 4, only the position error correction of the coordinate original point was explained as an example, but a correction of the joint angle can also be made in the same manner.

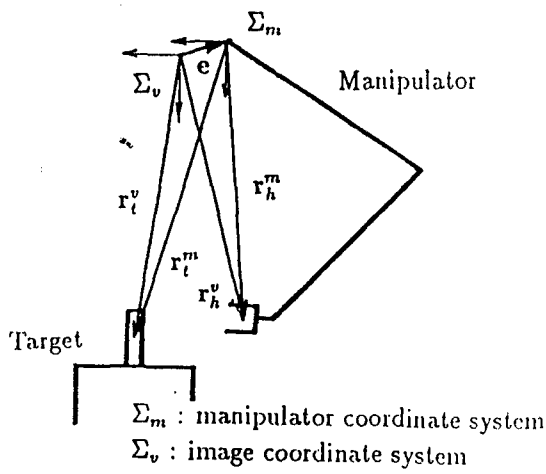

Fig.4. Compensation of Position

3. Trajectory Control of the Manipulator With Visual Information

In regards to the hand position, approach to the TS is in the sequence of the initial position O → A → B → C as shown in Fig. 5.

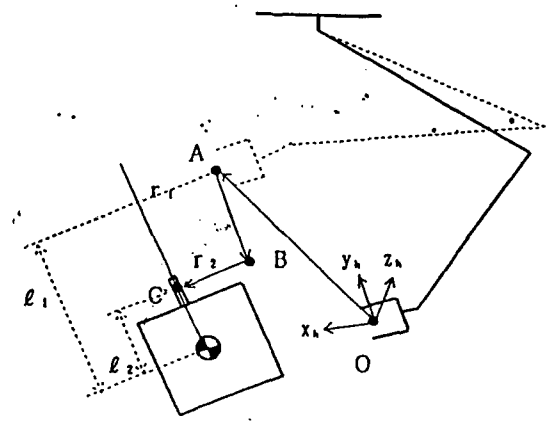

Fig.5. Trajectry of the Manipulator

In the process of O → A → B, information obtained from the EKF is used only in approach, and correction is made at the point B using the method described in 2.3.

In the process B → C, the correction value is fixed and this value is added to the EKF output for control. At the last point of C, the compliance control is made using a force/torque sensor at the hand tip to capture the target by absorbing the estimated error of the visual system. For a trajectory toward the command value, the current hand position r_h and target value (e.g., r_A, etc.) are connected with a straight line and a command proceeding at a constant speed on the line given. As an estimated value of the TS gravitational point r_g is sent from the visual system every 0.5 (approx.) seconds, the trajectory is modified each time the value is sent.

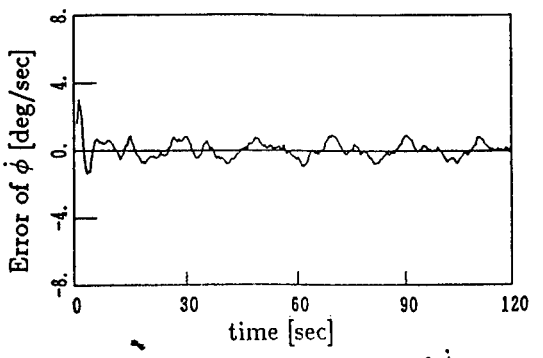

Fig.7. Estimation Error of $\dot{\phi}$

The attitude trajectory is modified likewise but its control is set to be insensitive to the rotation around the axis of the TS capturing rod as the rod is related to the axis.

In the tracking control to the set trajectory, the position and attitude errors of the hand tip are fed back to the angular velocity of each joint using the Yacobian matrix.[2]

In the control rule of this manipulator, an influence of the robot movement in reaction to the manipulator is not considered. However, it was possible to capture the TS by modifying the trajectory continuously from the images when the TS movement velocity is low.

4. Experiments

We have conducted experiments to verify the EKF property and to ascertain if the manipulator can be controlled accurately by the image information. For the experimental instruments, refer to the reference material.[1]

4.1 Recognition experiment of the movement using EKF

We have tried to recognize TS in nutation movement about 120 m away from the camera. We set the angular momentum vector in the z axis direction and the

angle at 20°, between the angular momentum vector and the TS's maximum inertial main axis. The spin and nutation rates were set to be about 3 rpm. The initial values of the position and attitude were from values from a triagonometrical survey and the speed was set at 0. For the EKF, 12 variables shown in the formula (1) are estimated and one of their examples is shown in Fig. 6 and 7: an estimated value of $\dot{\phi}$ (time differentiation of the Euler angle around the x axis) and its error. It is known that it is converged after about 10 seconds and estimation is made stable since then. After the convergence, a steady error still remains but this is due to an error of initial settings, etc. in the visual system.

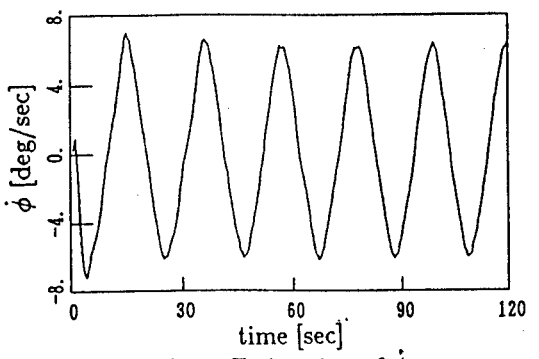

Fig.6. Estimation of $\dot{\phi}$

4.2 Capturing experiment

We have conducted capturing experiment with varied parameters. Its results will be introduced in videos. In the experiment, we could move the hand almost accurately to a position of the TS capturing rod and track down the rod with the hand. Further, by adding the compliance control, the capturing rod was held without giving an unnatural force to the hand tip. There were variances in some cases but correction was made about 1 to 3 cm using the light source attached to the hand.

5. Conclusion

We have proposed here a TS recognition method using visual information, a manipulator control method based on its information obtained from processing the recognition, and have conducted an experiment of capturing the target in a state simulating a relative motion in the weightless space on a simulator device. As a result, we have verified that it is possible to capture TS steadily, even in a state of floating in weightless condition using these methods.

From now on, we are going to check various other recognition and control methods and, while evaluating them using simulation devices, improve capability of the devices to cover more simulation cases. In conclusion, we would like to thank Mr. Katsuhiko Yamada for his advice in the processing algorithm and Messrs. Yoshigi Yabuuchi and Kazuhiko Fukushima for their cooperation in designing and manufacturing the experiment devices - all from Mitsubishi Electric Corporation.

References

[1] Shimochi, et al., "Development of a Simulator Device for Re-use Experiments", Space AI, Robotics and Automation Symposium, 1988.

[2] Inoue, "Work Coordinate Feedback Control of a Manipulator having Joints with Feed-back Velocity", Automated Instrument Control Society Journal, Vol 24, No 9, 1988.

A Study on Functional Allocation of Robot Systems in Orbit

906C0047 Tokyo SAIRAS 89 PROCEEDINGS in Japanese 18-19 Oct 89 pp 214-222

[Article by Yuuki Yoshie and Fumiaki Sano of the Space Station Department, Ishikawajima-Harima Heavy Industries Co., Ltd.]

[Text] Abstract

The needs for the space robot systems are increasing all over the world. They are expected to support platforms or space factories deployed in the space infrastructure based on the Space Station Freedom around the turn of the century.

The study on the functional allocation of robot systems is important, because many kinds of systems in orbit involving the space robots may be considered.

In this report, the mission analyses, the system studies and the study on the functional allocation were carried out on the space systems in orbit involving the space robots, sponsored by the National Space Development agency of Japan.

Missions of space robots were extracted every space crafts which will be necessary for space infrastructure from 2000 to 2010. The intensity of necessity, the year and the frequency of every extracted missions were discussed.

Categorization of space systems was performed using 5 criteria such as moving ability, working environment, ability to perform plural missions, autonomous level and ability to carry massive objects. And 56 configurations of space systems were considered by means of the extracted characteristics of space systems belong to each of the categories.

The study on the functional allocation of the space systems were performed to minimize the cost per performance in space development, and a proposal how to develop the space robots was offered.

1. Introduction

The need for orbital robot systems is mounting worldwide as the support equipment to operate effectively and safely the space infrastructure. This infrastructure includes space factories and various platforms to be

deployed from the second half of 1990s with the space station Freedom as the core.

Missions to be performed by these orbital robot systems are varied and diversified and orbital robot systems for each mission need to have various configurations. Therefore, in deciding what kind of an orbital robot system should be developed, it is important to calrify the following points.

(1) What the robot system in orbit should do? (Discussion on missions)

(2) What kind of a configuration should be possible for the robot system in orbit? (Discussion on system candidate)

(3) What should be done by what system? (Discussion on functional distribution)

This paper will report an outline of the above discussions conducted in the "Study (No 2) of the Space Robot Technology" commissioned by the National Space Development Agency of Japan.

2. Discussion on Missions

2.1 Setting of a spacecraft for mission services

The space station Freedom will be launched for service in the second half of the 1990s. The period when orbital robot systems will be put to practice is assumed to be around 2000 and their service life is expected to be 10 years. A representative spacecraft served by orbital robot systems needed in 2000 to 2010 is picked up from the space infrastructure as the prerequisite for the discussion here. (Table 1).

Table. 1 Assumed Spacecrafts Served by Space Robot Systems

Served Spacecraft	Operation Starting Year	Typical Mission
ATP	2000	Space Experiment, Observation
COP	2006	Semi-Conductor Production
MSPF	2006	Acquisition of Manned Technology
JPOP	1998	Earth Observation
GPF(4t)	2002	Broadcasting
GPF(8t)	2007	Broadcasting
GEOP(4t)	2003	Earth Observation
SSF Phase1 Phase2	1998 2002	Space Experiment, Observation Base of Manned Space Activity
Conventional Satellite	Not Designed to be served by Robots in orbit Broken Satellites may be tumbling.	
Debris	Increasing in orbit by human space activity	

Note) ATP :Application Technology Platform
COP :Co-Orbiting Platform
MSPF:Manned Service Platform
JPOP:Japanese Polar Orbiting Platform
GPF :Geostationary Platform
GEOP:Geostationary Earth Observation Platform
SSF :Space Station Freedom

Table. 2 The missions of space robot systems

Robot Mission	N	F	Y
• Experiment/Production etc.	◎	◎	○
• Replacement of ORUs	◎	○	○
• Resupply of fuel/materials	◎	○	○
• Recovery of samples/products	◎	○	○
• Transportation	◎	○	○
• Inspection	◎	◎	○
• Repair	○	●	○
• Berthing/Docking of other spacecrafts	◎	○	○
• Assembly in orbit (COP only)	◎	△	△
• Towing (COP only)	◎	△	△

Note) N (Nesessity) ◎ : Nesessary、○ : Maybe Nesessary
F (frequency) ◎ : Always、○ : Sometimes、△ : Rare、● : Contingent
Y (year) ◎ : ~2000、○ : 2000~2005、△ : 2005~2010、× : 2010~

2.2 Picking up and streamlining of the missions

Missions of an orbital robot system for each service picked up in the above 2.1 are listed and we have streamlined the missions from three viewpoints - required degree, work frequency and required time.

As an example, missions for the co-orbiting platform (ATP,COP) are shown in Table 2.

3. Discussion on System

3.1 Categroization of orbital systems

Various systems with operational functions are categorized based on the following yardsticks. (Features of orbital systems in each category are picked up.)

(1) Shifting function: 3 ways
[Shifting in space/primary and secondary shifting/Fixation]

(2) Self-regulating level: 3 ways
[Near distance remote control (or steering)/remote distance remote control (or partly self-regulating)/self-regulating (or automation)]

(3) Generalization level: 2 ways
[Exclusive/general]

(4) Work environment: 2 ways
[Exposed environment/Pressurized environment]

(5) Carriable weight: 3 ways
[Small (~600 kg)/middle (600 kg ~5 tons)/large (5 tons~)]

Each system in orbit will be classified into 108 (3 x 3 x 2 x 2 x 3) categories in total.

3.2 Discussion on orbital system candidates

From among the 108 categories, some viable ones are picked up and from among the orbital systems belonging to each category, representative ones which seemed necessary by 2010 were selected.

4. Discussion on Functional Distribution among Orbital Robot Systems

Based on studies regarding the technical level that may become necessary for each orbital system, the basic policy was set and there was discussion on the functional distribution. There are many systems capable of carrying out each work. For example, services such as replace and supply on the co-orbiting platform (COP) are possible either by an orbital service vehicle (OSV), which is a space shifting type general-purpose robot system or by a general-purpose (fixed type or truss shifting type) manipulator on the co-orbiting platform.

Carrying works on the co-orbiting platform are possible either by an orbital service vehicle which is a general-purpose robot system or by a HOPE STS (space shuttle) which is a dedicated transportation system.

As to the policy of the functional distribution among systems, there are two main ideas - functions intensive method and functions distributed methods. The following is an advantage and disadvantage of each method.

(1) Functions intensive method

It is a method to concentrate as many functions as possible in a system. For example, it is possible to concentrate functions in an orbital service vehicle which is a space shifting type general-purpose robot.

The advantage of this functions intensive method is its dispensing with robot systems (dedicated/general) in many services, once a single high-function general-purpose robot system is available. Its disadvantage is a high technical level requirement for the high-function general-purpose robot system and a possibility of critical damages when the system fails.

(2) Functions distributed method

This is a method to distribute functions to many systems. For example, each servicing platform has its own general-purpose manipulator system and services (replacement, supply, etc.), made by itself. The advantage of this functions distributed method is to localize a system failure without affecting the entire system and each system does not need so much high technical level.

Its disadvantage is a requirement of many systems (dedicated/general).

The function distribution among systems can be summarized as in the foregoing ideas but, from a viewpoint of maximizing the cost-performance in space development, the optimum solution may be found midway between these methods.

Therefore, it will be important more than ever to come up with a rational role sharing between many dedicated and general-purpose systems.

5. Role Sharing of General-purpose and Dedicated Robot Systems (Examples)

We would like to introduce a replacement work of the mission payload in the JEM (Japanese Experiment Module) exposure section to be attached to the space station Freedom, now under development, as an example of the role sharing between general-purpose robot system and dedicated system.

The replacement work of the mission payload in the JEM exposure section is exercised in a cooperative work between the JEMRMS which is a manipulator of near-distance remote control type with 6-degree of freedom and the equipment exchange unit (EEU),[1] which is a dedicated system with 1-degree of freedom (Fig. 1).

The JEMRMS is mainly engaged in carrying the mission payload and in rough positioning.

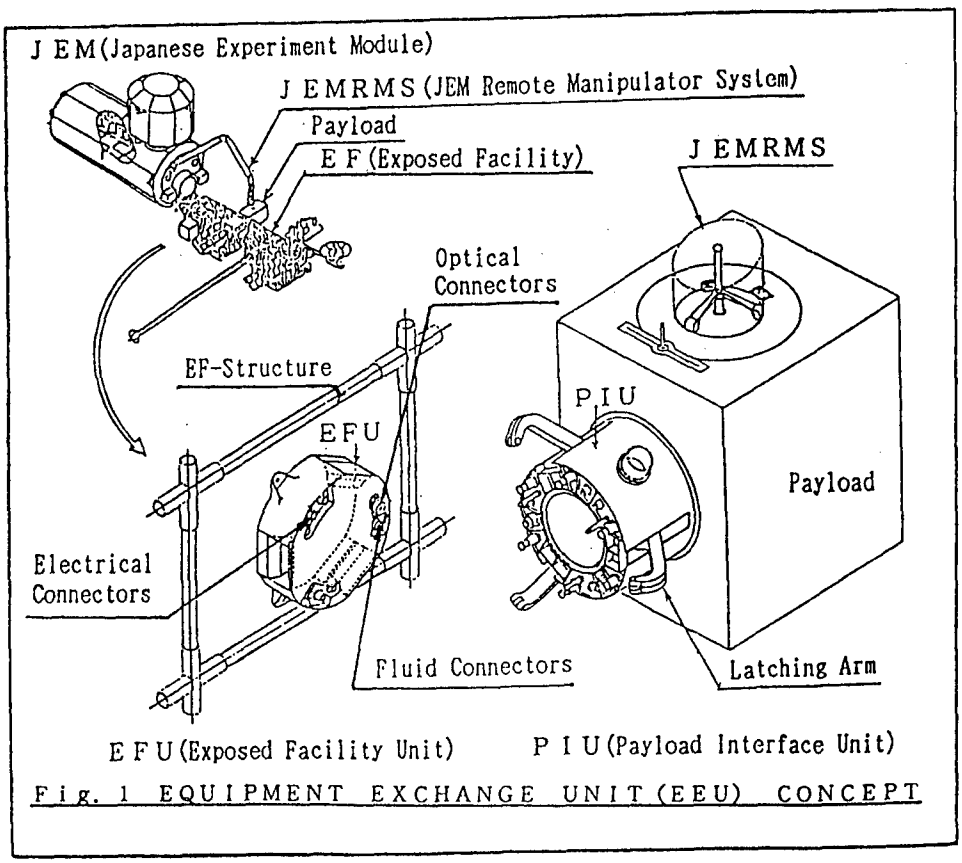

Fig. 1 EQUIPMENT EXCHANGE UNIT (EEU) CONCEPT

The equipment exchange unit is mainly dedicated to attaching and removing the mission payload to and from the exposure section structure. The following functions, not available with the JEMRMS, are realized with its light and compact unit.

(1) Tracking down and aligning functions in correcting an error of the JEMRMS positioning.

(2) Coupling and separation functions between the mission payload and the exposure section structure.

(3) Batched attaching and detaching functions of the interface elements such as the fluid couplers, electrical connectors, etc.

6. Conclusion

As symbolized in the space station project, it is now difficult to conduct a space development which needs a massive development investment by a single country and global role sharing is becoming more necessary toward the 21st century.

Among such roles, orbital robot systems which are being recognized significantly by nations all over the world are a field where Japan is comparatively good at making the most of her robotics technology on the ground. Positive promotion of this field is hoped for. The work missions in orbit are very diversified and extensive and, for an orbital system to implement them, a variety of its configurations are possible from a general-purpose high-function robot system to a light and compact dedicated system.

The vigorous function allocation among systems requires a re-examination when served missions, contents, technical levels required for each system, failure probabilities, etc. are clarified.

In developing the orbital robot systems from now on, it is considered necessary for Japan to study not only general-purpose high-function robot systems, but also various dedicated systems in parallel from a viewpoint of the maximum cost performance in space development. We would like to thank the National Aeronautics Development Agency of Japan who guided us in this discussion.

7. References

[1] Hattori, et al., "R & D of an Equipment Exchange Unit of the Exposure section", 5th Space Station Symposium Journal, pp 51-52, 1989.

A Teleoperating Assembly System

906C0047 Tokyo SAIRAS 89 PROCEEDINGS in Japanese 18-19 Oct 89 pp 264-267

[Article by Hajime Morikawa, Nobuaki Takanashi, Norio Tagawa and Hiroshi Fukuchi - NEC Corporation C&C Systems Research Laboratories]

[Text] Abstract

In the near future, it will be important to develop space robotic systems for assembly tasks, inspections and maintenance work. As the first step in developing autonomous space robotic systems, a teleoperating assembly system for use in the space environment has been developed.

In this system, a new target mark is proposed to guide the object easily by a human operator using a manipulator. In addition, a real-time simulator is used with every operation, so that the operator can easily understand the assembly environment and avoid obstacles without an actual manipulator motion. In order to verify this teleoperating system effectiveness, assembly experiments were carried out using an assembly type lager-scale space antenna. Results indicated that it was possible for an operator to assemble the antenna easily using the system. The experiments proved that the positioning accuracy using this target mark was sufficient for this antenna assembly.

The system is composed of a teleoperating console, a real-time simulator, a robotic manipulator, a robot controller, a target mark and a CCD camera. A new three-dimensional target mark, which is attached to the target object, is used to measure the object position along six-degrees of freedom directions. Positional differences can be detected by an operator with the target mark image change. The operator controls the manipulator using a teleoperating console, so that the current target mark image matches the reference target mark image, which corresponds to the final target position. This teleoperating console has an image processor to extract mark image features.

A real-time simulator was used to check both the manipulator motion and collision with obstacles. The simulator shows the manipulator motion, using the desired position data from the console. After the operator checks the manipulator motion, a motion command is sent to the robot controller. This simulator can also be used for off-line trajectory planning or making teaching data.

The positioning accuracy using the target mark was investigated experimentally. The image processor extracted position information from binary mark images. The mark position data, when the image was acquired, was recorded and the displacement between the mark position and the reference position was calculated. Using these data, the accuracy for positioning error detection was measured. The experimental results show that the positioning accuracy using this mark is sufficient for general assembly tasks.

The authors have also developed a new sensor integrated space antenna for assembly experiment use. This space antenna consists of an antenna body and eight separate antenna segments. The antenna body is equipped with a connection mechanism, the CCD camera and a light source. Each separate antenna segment has a target mark. Connection mechanisms were developed to make assembly simple.

The antenna assembly experiments were carried out and experimental results proved that the visual information from the mark image made the antenna assembly operation easy. Also the results showed that the simulator was useful for both checking human operation error and helping the operator to understand the environment.

Though the effectiveness of this system was verified, some problems, such as automatic obstacles avoidance, the vibration problem in space structures and applying a compliance control method, still remain unsolved. Now the authors are making efforts to improve positioning accuracy using visual information and to add intelligence to the assembly system.

1. Introduction

In this paper, we have supposed an assembly work in space as the basic discussion of a robot system performing assembly, check and repair required on a space station, and developed a remote control robot system using visual information. The system validity was verified by evaluating the positioning accuracy with the visual image processing, and applying an assembly of the parabola antenna for space.

2. Remote Control System

This system is an experimental system on the ground, which is supposed to do an assembly operation in space by an operator with a remote control of multi-joint arm. It is excellent in extendability and has the following features.

- o Guiding for positioning with 6 degrees of freedom with mark images
- o Automated extraction of the mark feature quantity with the image processing
- o Display of the work state in real-time simulation
- o Operation check and off-line teaching functions

The remote control is conducted by observing a new cubic mark set at the segment facing the operation, and aligning the mark image shape to the reference image extracted from the mark image features after assembly.

Once a real-time arm operation and position relationship among operation objects are displayed in simulation, and their operations are ascertained then the arm operation is conducted. With the above methods, the operator is allowed to watch the mark image and simulation display to complete the assembly operation by positioning guidance of 6-degree freedom without supervising the real arm operation.

An example of the system configuration is shown in Fig. 1 when this system is applied to an antenna assembly operation.

A cubic mark is set at the separate antenna segment that is to be operated and, with the CCD camera set on the antenna body, the mark image can be picked up. The remote control console is capable of a superimposed display of the mark's camera image and the reference image on its CRT. Therefore, while watching the display, the remote control is possible using a joystick or the like. Further, its features include extraction of features of a mark, and image processing functions, such as the positioning attitude measurement. The real-time simulator is linked with the remote control console connected by GRIB and displays in real-time, a simulation of the assembly operation. It is also possible to display from any optional direction based on the viewpoint data. Furthermore, it has off-line orbital planning and teaching functions. For calculation, DSP[1] is used for the high-speed real-time operation processing. For the arm, a 6-degree freedom vertical multi-joint type is used.

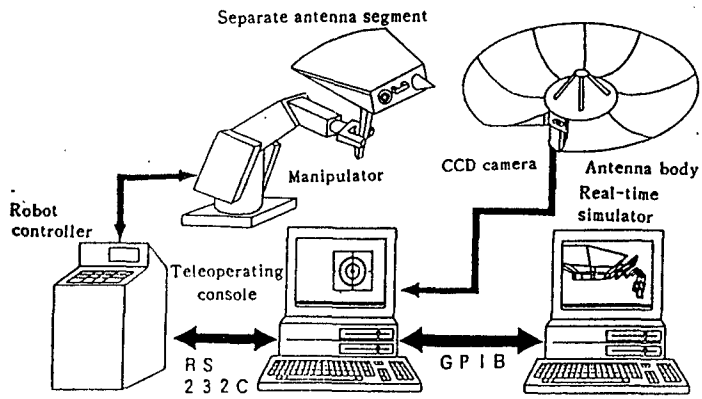

Fig.1 Teleoperating system block diagram

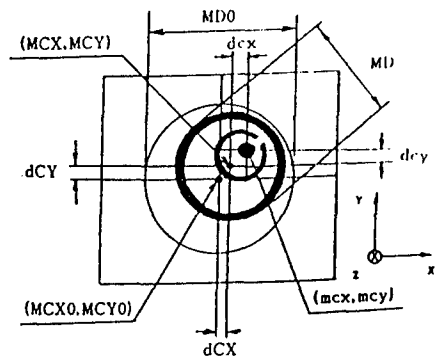

Fig.2 Mark image feautures

3. Positioning Mark

3.1 Features of the mark

The largest feature of this system is to guide positioning using a three-dimensional positioning mark. This mark has the following features.

- o Easy to use detection for 6-degree freedom positioning and attitude errors
- o Easy to understand features of a mark and simple image processing
- o With its dented shape, it is possible to be set to the joining face of an assembly target.

As to the method for detecting a positioning error, we would like to explain an example using features of a mark shown in Fig. 2 and binary images of an actual mark shown in Fig. 3.

Fig. 3 (a) is a case when a mark is on the reference position. It is observed that, starting from the mark center in sequence, a concentric circle is formed by a central circle with a cross, mid ring with a notch and circumference ring at the outside.

This is because the mark has a structure mortised in a concentric circle from the observation direction. Fig. 3 (b) shows when a parallel progress (translation) displacement is given in the z-axis direction. With a mark center position (MCX0,MCY0) on the reference position as a center, and the outer ring of MD0 in diameter is superimposed as the reference image, the mark diameter has a difference (MD-MD0) though the shape is similar, making it possible to estimate a displacement in the Z-axis direction. Fig. 3 (c) is a case when a rotation displacement is given around the X-axis further. When the center (mcx,mcy) of the central circle and the center position (MCX,MCY) of the circumference ring are noticed, a dislocation dcy (mcy-MCY) is caused and this change is used as a reference to estimate the rotation quantity.

Fig. 3 (d) is a case when a parallel progress displacement is given to Fig. 3 (c) in the Y-axis direction, this can be estimated from a difference dCY (MCY-MCYO) caused between the center position (MCX,MCY) of the outer ring and the center position (MCXO,MCYO) of the reference image. The Y-axis direction is estimated likewise and a change of the notch of the mid ring is used as a reference around the Z-axis and it is known that position errors in 6 free degrees in total can be detected. Further, in a general case when these displacements are combined, it is possible to detect a position error through proper procedure.

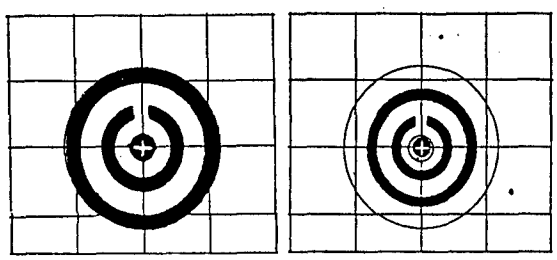

(a)Reference position (b)Displacement along Z-axis

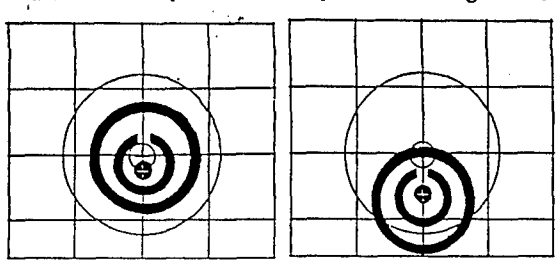

(c)Rotation around X-axis (d)Displacement along Y-axis

Fig.3 Binary mark images

3.2 Evaluation experiment of a position error detection accuracy

By extracting features of the mark described in the foregoing section through image processing, we have conducted a quantitative evaluation of position error detection accuracy.

For measurement, a mark of 50 mm in diameter and 40 mm in depth was used. We extracted feature quantities of mark images when a displacement is given to each degree of freedom with an arm remote control. The resolution of the processed images was 512 x 480 pixel. Position data for each image were recorded and a displacement quantity was calculated from the reference position. Above results were coordinated into a relation between displacements and mark features, part of which is shown in Fig. 4.

Fig. 4 (a) shows a change of the difference (dCX) between the center of the mark's outer ring and the center position of the reference image when a translation displacement is given only to the X-axis direction at a point dZ = 78.7 mm.

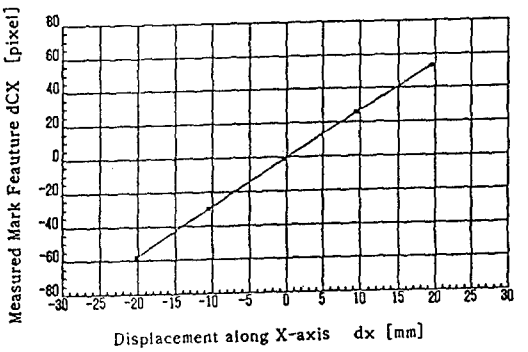

(a) Relation between dX and dCX

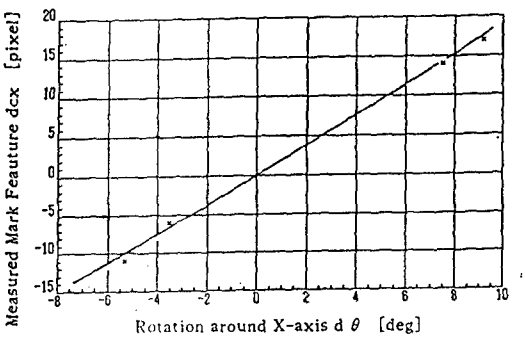

(b) Relation between d θ and dcx

Fig. 4 Experimental results

Fig 4. (b) shows a change of the difference (dcx) between the mark's center circle and the center position of the mark's outer ring when a rotation displacement dϕ is given around the X-axis at a point dZ = 57.7 mm. In both cases, a feature quantity for each given displacement is given in a straight line passing through the original point and a similar result was obtained for the Y-axis direction. It is also possible to estimate a position attitude for the Z-axis direction using features that a mark's diameter MD and distance dZ are in reverse proportion.

Measured accuracies in the proximity of dZ = 60 mm were as follows:

Along X and Y axes : $\pm$ 0.3 mm/pixel

Along X axis : $\pm$ 1.3 mm/pixel

Around X and Y axes : $\pm$ 0.5° /pixel

Therefore, we could detect position errors with very high accuracy.

4. Antenna Assembling Experiment

4.1 Assembly-type antenna

This system was used for an antenna assembling experiment testing for the effectiveness of the system, which was verified.

The assembly-type antenna used for this assembling experiment had a diameter of 2 meters with one central mirror and eight divided mirrors. Fig. 5 shows a junction plane of the central mirror and eight divided morrors. To make the assembly work easier, a latch mechanism and a positioning guide mechanism (boss, cone guide) are set up as the assembling mechanism. A CCD camera, ring light and mirror were set up as the optical units for guidance with mark images. Further, a compliance mechanism utilizing a spring was provided to the antenna holding section to absorb a position error due to the guide mechanism. With the CCD camera and ring light set inside the central mirror, images were picked up through the mirror and lighting was made possible.

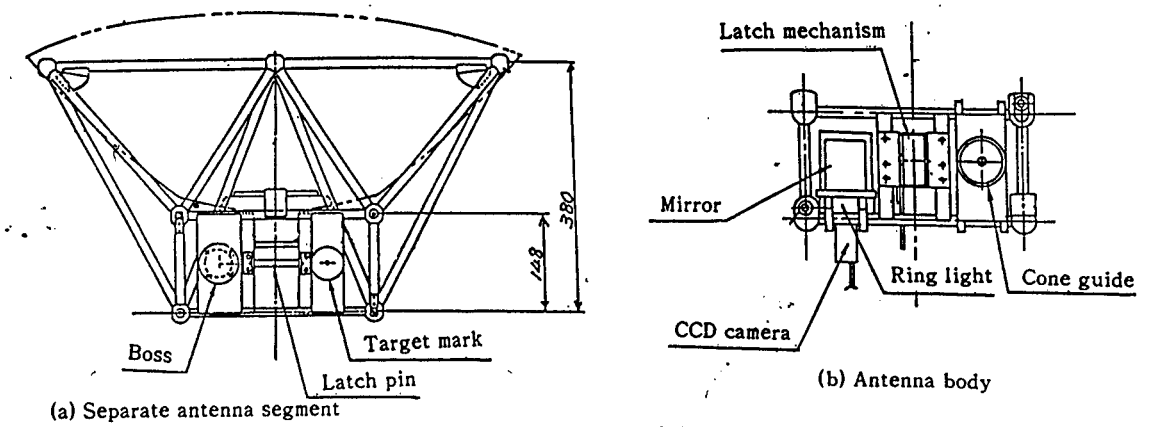

(a) Separate antenna segment

(b) Antenna body

Fig.5 Configuration of the space antenna

4.2 Results of the assembling experiment

Using the real-time simulator first, the teaching data were made off line and, based on these data, the divided mirrors were held and the arm was shifted within the field of view. In the field of view, the assembling experiment was conducted with remote control at a point about 20 cm away from the junction plane of the central mirror.

Fig. 6 shows a display example of real-time simulation and Fig. 7 shows its experiment sytem. As a result of the experiment, it was confirmed that the assembly completion guidance can be conducted favorably using the mark images. The real-time simulation was useful and effective in grasping an operation state and avoiding collision and breakdown of objects due to an error of the operator. Further, after guiding the mark with a specified range, it was confirmed that an assembly can be exercised easily by guiding only to the vertical direction facing the junction plane. The guidance and compliance mechanisms were effective.

5. Tasks to be Settled

We are studying a partly-self-regulating assembly, an assembling experiment considering the vibration problem in space and an assembling experiment applying the active compliance control.

(Acknowledgement) We would like to thank Mr. Takanori Ikeda of NEC Technical Information System Corp.

References

(1) Takanashi et al, "Application of DSP-based High-speed Operation Engine to a High-function Robot Controller", 2nd Space Artificial Intelligence/ Robotics/Automation Symposium, 1988, pp 115-118.

- END -

Foreign Broadcast Information Service (FBIS) and Joint Publications Research Service (JPRS) publications contain political, military, economic, environmental, and sociological news, commentary, and other information, as well as scientific and technical data and reports. All information has been obtained from foreign radio and television broadcasts, news agency transmissions, newspapers, books, and periodicals. Items generally are processed from the first or best available sources. It should not be inferred that they have been disseminated only in the medium, in the language, or to the area indicated. Items from foreign language sources are translated; those from English-language sources are transcribed. Except for excluding certain diacritics, FBIS renders personal names and place-names in accordance with the romanization systems approved for U.S. Government publications by the U.S. Board of Geographic Names.

Headlines, editorial reports, and material enclosed in brackets [ ] are supplied by FBIS/JPRS. Processing indicators such as [Text] or [Excerpts] in the first line of each item indicate how the information was processed from the original. Unfamiliar names rendered phonetically are enclosed in parentheses. Words or names preceded by a question mark and enclosed in parentheses were not clear from the original source but have been supplied as appropriate to the context. Other unattributed parenthetical notes within the body of an item originate with the source. Times within items are as given by the source. Passages in boldface or italics are as published.

SUBSCRIPTION/PROCUREMENT INFORMATION

The FBIS DAILY REPORT contains current news and information and is published Monday through Friday in eight volumes: China, East Europe, Soviet Union, East Asia, Near East & South Asia, Sub-Saharan Africa, Latin America, and West Europe. Supplements to the DAILY REPORTs may also be available periodically and will be distributed to regular DAILY REPORT subscribers. JPRS publications, which include approximately 50 regional, worldwide, and topical reports, generally contain less time-sensitive information and are published periodically.

Current DAILY REPORTs and JPRS publications are listed in *Government Reports Announcements* issued semimonthly by the National Technical Information Service (NTIS), 5285 Port Royal Road, Springfield, Virginia 22161 and the *Monthly Catalog of U.S. Government Publications* issued by the Superintendent of Documents, U.S. Government Printing Office, Washington, D.C. 20402.

The public may subscribe to either hardcover or microfiche versions of the DAILY REPORTs and JPRS publications through NTIS at the above address or by calling (703) 487-4630. Subscription rates will be provided by NTIS upon request. Subscriptions are available outside the United States from NTIS or appointed foreign dealers. New subscribers should expect a 30-day delay in receipt of the first issue.

U.S. Government offices may obtain subscriptions to the DAILY REPORTs or JPRS publications (hardcover or microfiche) at no charge through their sponsoring organizations. For additional information or assistance, call FBIS, (202) 338-6735,or write to P.O. Box 2604, Washington, D.C. 20013. Department of Defense consumers are required to submit requests through appropriate command validation channels to DIA, RTS-2C, Washington, D.C. 20301. (Telephone: (202) 373-3771, Autovon: 243-3771.)

Back issues or single copies of the DAILY REPORTs and JPRS publications are not available. Both the DAILY REPORTs and the JPRS publications are on file for public reference at the Library of Congress and at many Federal Depository Libraries. Reference copies may also be seen at many public and university libraries throughout the United States.